University of Crete
School of Science and Engineering
Department of Biology

Foundation for Research and Technology- Hellas (FORTH)
Institute of Molecular Biology and Biotechnology (IMBB)
Laboratory of Neurogenetics and Ageing

The role of epigenetic factors on metabolism in the nematode *Caenorhabditis elegans*

Magdalene Giannopoulou
Student Registration Number: 3248

Scientific supervisor
Nektarios Tavernarakis

Academic supervisor
Daphne- Maria Bazopoulou

Heraklion, October 2023

Η εν λόγω πτυχιακή εργασία εκπονήθηκε στο εργαστήριο «Νευρογενετικής και Γήρανσης» υπό την επίβλεψη του καθηγητή Νεκτάριου Ταβερναράκη στο Ινστιτούτο Μοριακής Βιολογίας και Βιοτεχνολογίας (IMBB) του Ιδρύματος Τεχνολογίας και Έρευνας (FORTH).

Στην οικογένειά μου,

Σπύρος, Βαρβάρα, Δημήτρης

Στους φίλους μου

Acknowledgments- Ευχαριστίες

Ένας ολόκληρος χρόνος προσωπικής και ακαδημαϊκής ανέλιξης έφτασε στο τέλος του με τη συγγραφή ετούτης της πτυχιακής εργασίας. Με το κλείσιμο αυτού του κεφαλαίου σημαίνεται επίσημα το τέλος των προπτυχιακών μου σπουδών στο Τμήμα Βιολογίας του Πανεπιστημίου Κρήτης, μα συνάμα και ένα νέο ξεκίνημα στην μετέπειτα εκπαιδευτική μου πορεία. Φυσικά, αυτό το εγχείρημα δεν θα ήταν δυνατό χωρίς την αταλάντευτη υποστήριξη και καθοδήγηση αξιόλογων ανθρώπων που είχα την τύχη να βρίσκονται στο πλευρό μου.

Νιώθω βαθύτατα ευγνώμων που αποτέλεσα μέλος της ομάδας του κύριου Νεκτάριου Ταβερναράκη και τον ευχαριστώ από καρδιάς που μου έδωσε την ευκαιρία να ζήσω μια σπουδαία επιστημονική εμπειρία στο εργαστήριό του, η οποία αποτέλεσε πρόσφορο έδαφος για να ευδοκιμήσει το ενδιαφέρον μου για την έρευνα. Η δυνατότητα αυτή είναι καθοριστική για την πραγμάτωση φιλόδοξων μελλοντικών πλάνων στον ακαδημαϊκό χώρο. Ένα μεγάλο ευχαριστώ αναλογεί, επίσης, στην κυρία Δάφνη- Μαρία Μπαζοπούλου, που είχε την ευγενική διάθεση να συνεπιβλέπει, ως μέλος ΔΕΠ του Τμήματος Βιολογίας, την παρούσα πτυχιακή εργασία.

Εν συνεχεία, θα ήθελα να ευχαριστήσω θερμά την πρώτη supervisor μου Χριστίνα Πλουμή, η οποία με πολλή προθυμία με καθοδηγούσε υπομονετικά κατά τα αρχικά μου βήματα στο εργαστήριο. Οφείλω, επίσης, ένα ευχαριστώ στη δεύτερη supervisor μου Teresa Rubio-Tomás, για την επιστημονική επιμέλεια της πτυχιακής, την εποικοδομητική της κριτική και για τον καίριο ρόλο της στην έκβαση του project.

Δε θα μπορούσα να μην ευχαριστήσω την κα. Μαίρη Μαρκάκη, για την αμέριστη υποστήριξη και την πολύτιμη βοήθειά της τον τελευταίο χρόνο. Ευχαριστώ πολύ και την Αγγέλα Πασπαράκη, που πάντα μεριμνούσε για την τεχνική υποστήριξη των πειραμάτων μας.

Ευχαριστώ πολύ όλα τα μέλη του εργαστηρίου που δημιούργησαν ένα όμορφο, ευχάριστο και άκρως φιλικό κλίμα συνεργασίας. Τους ευχαριστώ για όλες τις χρήσιμες γνώσεις που μοιράστηκαν μαζί μου, αλλά και για τις γόνιμες συζητήσεις μας.

Τέλος, τα λόγια δεν μπορούν να περιγράψουν την ευγνωμοσύνη που αισθάνομαι για την οικογένειά μου. Χωρίς την αγάπη, την ενθάρρυνση και την εμψύχωσή τους, δεν θα κατάφερνα να φτάσω ως εδώ. Η πίστη τους στις δυνατότητές μου αποτελούσε πηγή κινήτρου για εμένα. Τους οφείλω κάθε μου επίτευγμα!

Σας ευχαριστώ,

Μάγδα

Table of Contents

1. Abstract in Greek- Περίληψη στα ελληνικά

Στον τομέα της μοριακής βιολογίας, η αιτιώδης σχέση μεταξύ των τροποποιήσεων της χρωματίνης και του μεταβολισμού των λιπιδίων έχει συγκεντρώσει σημαντική προσοχή. Η χρωματίνη, το ικρίωμα του γενετικού μας κώδικα, μπορεί να υποστεί πολλαπλές χημικές και δομικές αλλαγές, που είναι στενά συνυφασμένες με μεταβολικές διεργασίες. Οι διατροφικές συνήθειες και η πρόσληψη τροφής μπορεί να εισάγουν όχι μόνο απαραίτητα θρεπτικά συστατικά αλλά και επιγενετικούς ρυθμιστές, που δύναται να επηρεάσουν σημαντικά το επιγένωμα του οργανισμού. Είναι ενδιαφέρον ότι τα λιπίδια δεν χρησιμεύουν μόνο ως ζωτικές πηγές ενέργειας, αλλά δρουν και ως μόρια σηματοδότησης, ενορχηστρώνοντας μια πληθώρα κυτταρικών μονοπατιών και επηρεάζοντας διάφορες φυσιολογικές διεργασίες. Ταυτόχρονα, τα λιπίδια διαμορφώνουν τον επιγενετικό έλεγχο του μεταβολισμού, δημιουργώντας έναν κύκλο ανατροφοδότησης, όπου ο μεταβολισμός κατευθύνει την τύχη των λιπιδίων, η οποία στη συνέχεια επηρεάζει αμοιβαία τις επιγενετικές τροποποιήσεις, διατηρώντας έναν κύκλο δυναμικής ισορροπίας. Παρά την αυξανόμενη κατανόηση αυτής της αλληλεξάρτησης, ο ρόλος συγκεκριμένων επιγενετικών παραγόντων στη ρύθμιση των γονιδίων που σχετίζονται με τη μεταβολική επεξεργασία των λιπιδίων, ιδίως των μονοακόρεστων λιπαρών οξέων, παραμένει ένας τομέας που χρήζει βαθύτερης διερεύνησης. Στην εν λόγω μελέτη, χρησιμοποιούμε στελέχη *C. elegans*, συμπεριλαμβανομένου του άγριου τύπου N2 και στελέχη knockout για συγκεκριμένους επιγενετικούς ρυθμιστές, ώστε να διερευνήσουμε τις επιδράσεις μιας διατροφής υψηλής περιεκτικότητας σε λιπαρά οξέα στη μακροζωία και στη μιτοχονδριακή ομοιόσταση. Υπό συνθήκες διατροφής υψηλής περιεκτικότητας σε λιπαρά οξέα, το στέλεχος N2 παρουσίασε μειωμένη μέση διάρκεια ζωής, ενώ τα στελέχη knockout εμφάνισαν ανθεκτικότητα. Επιπλέον, τα μεταλλαγμένα στελέχη εμφάνισαν σημαντική μείωση των επιπέδων μιτοχονδριακών δραστικών ειδών οξυγόνου κατά την παροχή διατροφής υψηλής περιεκτικότητας σε λιπαρά, σε αντίθεση με το στέλεχος N2. Οι παρατηρήσεις αυτές, αν και εύστοχες, αντιπροσωπεύουν μόνο ένα κομμάτι ενός ευρύτερου επιστημονικού αινίγματος γύρω από τον μεταβολισμό και την επιγενετική. Η αποκάλυψη αυτών των μηχανισμών θα μπορούσε ενδεχομένως να οδηγήσει στην ανάπτυξη νέων θεραπευτικών προσεγγίσεων που στοχεύουν σε πολλαπλές μεταβολικές διαταραχές, όπως η παχυσαρκία και οι δυσμενείς επιπτώσεις της.

2. Abstract

In the field of molecular biology, the causal relationship between chromatin changes and lipid metabolism has gathered significant attention. Chromatin, the scaffold of our genetic code, can undergo multiple chemical and structural modifications that are tightly intertwined with metabolic processes. Dietary habits and food intake may introduce not only essential nutrients but also epigenetic modulators, that can greatly impact the epigenetic landscape of the organism. Interestingly, lipids do not only serve as vital energy reservoirs, but also act as signaling molecules, orchestrating a plethora of cellular pathways and influencing various physiological processes. Concomitantly, lipids modulate epigenetic control of metabolism, creating a feedback loop, wherein metabolism directs lipid fate, which then reciprocally affects epigenetic modifications, sustaining a cycle of a dynamic equilibrium. Despite the growing understanding of this interdependence, the role of specific epigenetic factors in regulating genes associated with metabolic processing of lipids, in particular monounsaturated fatty acids, remains an area warranting deeper exploration. Here, we recruit *C. elegans* strains, including N2 wild-type and epigenetic regulator knockouts, to investigate the effects of a high-fat diet on longevity and mitochondrial homeostasis. Under high-fat dietary conditions, the N2 strain exhibited reduced mean lifespan, whereas the knockout strains showed resilience. Additionally, mutant strains displayed a significant reduction in mitochondrial reactive oxygen species levels upon high-fat diet treatment, contrary to the N2 strain. These observations, while insightful, represent only a fragment of a broader scientific enigma surrounding metabolism and epigenetics. Unraveling these mechanisms could potentially lead to the development of novel therapeutic approaches targeting multiple metabolic disorders, like obesity and its adverse effects.

3. Abbreviations in alphabetical order

ANOVA= Analysis of Variance

CRISPR/Cas 9= Clustered Regularly Interspaced Short Palindromic Repeats- Caspase 9

daf-16= decay-accelerating factor 16 gene

daf-2= decay-accelerating factor 2 gene

DTC= distal tip cell

EMS mutagenesis= Ethyl methanesulfonate mutagenesis

GFP= Green Fluorescence Protein

HATs= Histone Acetyltransferases

hda-2= histone deacetylase 2 gene

HDAs= Histone Deacetylases

HDMs= Histone Demethylases

HFD= High- Fat Diet

HKMTase= Histone Lysine Methyltransferases

HMTs= Histone Methyltransferases

hsf-1= heat shock factor 1 gene

KMTs= Lysine Methyltransferases

KO= knockout

LoxP= locus of X-over P1 site

MUFAs= Monounsuturated Fatty Acids

NAFLD= Non-Alcoholic Fatty Liver Disease

neoR= neomycin resistance

ORF= Open Reading Frame

ROS= Reactive Oxygen Species

RT- qPCR= Real Time quantitative Polymerase Chain Reaction

RT= Room Temperature

S/MARs= Scaffold/ Matrix Attachment Regions

SAMs= S-adenosyl methionine

set-14= SET-domain containing methyltransferase gene

set-18= SET-domain containing methyltransferase gene

set-30= SET-domain containing methyltransferase gene

set-4= SET-domain containing methyltransferase gene

skn-1= skinhead 1 gene

sod-3= superoxide dismutase 3 gene

TADs= Topologically Associated Domains

UTR= Untranslated Region

4. Introduction

4.1. *Caenorhabditis elegans*

4.1.1. Biological characteristics of the nematode *Caenorhabditis elegans*

Caenorhabditis elegans, commonly referred to as *C. elegans*, is a species belonging to the Phylum Nematoda, which was first identified and described by Émile Maupas in 1900. [1] Since then, *C. elegans* has undergone extensive nomenclatural and taxonomic alterations, evolving from a relatively obscure nematode species to a central model organism in modern biological research. It wasn't until 1974 that *C. elegans* was established as a useful model organism for neurodevelopmental biology and the study of genetics. [2]

C. elegans is a tiny non-parasitic multicellular organism, measuring approximately no more than 1 mm in size and 0.1 mm in diameter (adult animals). The nematode resides in the soil, occupying niches enriched in microorganisms, as it is bacterivorous. This suggests that its principal source of nutrition are various bacterial strains found naturally in its surroundings. [3] For experimental purposes in the laboratory, *C. elegans* feeds monoxenically on *Escherichia coli* wild-type bacterial strain OP50, cultured in Luria-Bertani (LB) medium. [4] *E. coli* OP50 bacteria exhibit a uracil auxotrophy phenotype and a restricted growth on NGM (Nematode Growth Medium) plates. [5] After seeding NGM plates with liquid OP50 bacterial culture, worms can be placed on top of the lawn and maintained at a consistent temperature, typically at 20°C. [3]

Despite displaying a rather simple structure compared to other multicellular organisms, *C. elegans* appears to have a well-organized anatomy [6], adapted to efficiently support the nematode's range of functions. The hermaphrodite *C. elegans* precisely consists of 959 somatic cells, whereas for its male counterpart the number rises to 1031. [3]

Five major types of tissues collectively make up for the nematode's cylindrical body *(Figure 1)*. The hypodermis consists of cellular layers that cover the worm externally, providing it with the necessary structural support and protection from dehydration. Underlying hypodermal cells secrete a plethora of substances, such as cross-linked collagens and glycoproteins that line the worm's exterior. This matrix is known as the cuticle and, similar to mammalian skin, constitutes a physical barrier by impeding environmental stresses (e.g. chemicals, UV radiation, etc.) from entering the body. [6,7]

Underneath the hypodermis lies the muscle tissue, which is organized in longitudinal bands and circular rings. Muscle tissue allows not only for the sinusoidal locomotion of the worm, but is also critical for performing several functions, such as pharynx movements during bacterial grinding. [6,8,9] The worm's sensory and motor abilities are orchestrated by the neuronal tissue concentrated in the head and tail regions. Hermaphrodite and male nematodes have a total of 302 and 385 neurons, respectively. Extensive electron microscopy studies have been carried out in order to effectively charter the nematode's unique neuronal network. [3,6,10] Further within the nematode's body, the intestine is a tubular structure that extends from the mouth (anteriorly) to the anus (posteriorly). The intestine is responsible for multiple functions, including food digestion, nutrient absorption, excrement elimination, pathogenic avoidance, immunity and host defense. [6,11,12] Finally, the *C. elegans* gonad is a highly organized bilaterally symmetrical structure that plays a central role in reproduction. In hermaphrodites, the gonad produces both oocytes and sperm, with sperm production occurring during the larval stages and oocyte production dominating in adulthood. In contrast, male *C. elegans* animals have a simpler gonad that produces only sperm, which is used to fertilize hermaphrodite oocytes during mating. [13]

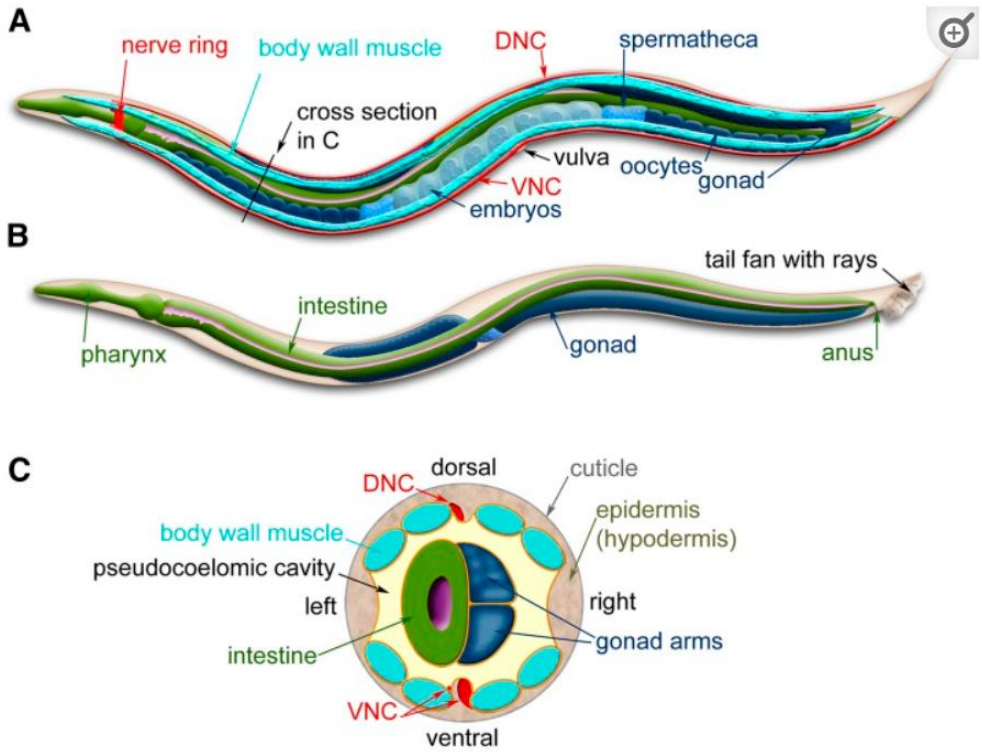

Figure 1 The internal tissues and structures in A. hermaphrodite and B. male nematodes. In section C. we observe a cross-section through the anterior region of the *C. elegans* hermaphrodite. DNC – Dorsal Nerve Cord, VNC – Ventral Nerve Cord. (Source: Corsi et al., 2015 – see references)

4.1.2. Reproductive system

The reproductive system of the nematode *C. elegans* has been a subject of extensive research due to its significance in understanding developmental biology and cellular mechanisms. Similar to most animals, from simple invertebrates to complex vertebrates, gonads constitute the primary reproductive organs where gametogenesis and fertilization can take place. [6,14]

Hermaphrodites have the ability produce both egg cells and sperm, making them able to either self-fertilize or cross-fertilize with other males to introduce genetic diversity. A wild-type N2 worm can produce approximately 300 offspring through self-fertilization and more than 1000 offspring when mated with a male. Hermaphrodite animals have two copies of the sex chromosome (XX) and are, thus, diploid. [3,4] The hermaphrodite gonad consists of two arms forming a U-shape structure. *(Figure 2)* Each arm contains a distal tip cell (DTC) that promotes the mitotic proliferation of germ cells. As these germ cells move away from the DTC, they enter meiosis and differentiate into oocytes. [6,15,16] Before oocyte production, hermaphrodites undergo a phase of sperm production. Sperm cells are stored in the spermatheca, a specialized organ, until they are used to fertilize the oocytes. [6] After fertilization, the zygote travels to the uterus and starts the process of embryonic growth. Apart from germ line cells, hermaphrodite gonad also consists of the somatic gonad. The somatic gonad in *C. elegans* combined with the gonadal sheath (layer of somatic cells that surround the germline), form a component of the reproductive system that provides structural support and plays a pivotal role in regulating germline development, by managing oocyte maturation, entry, and the exit of the fertilized embryo into the uterus. [15]

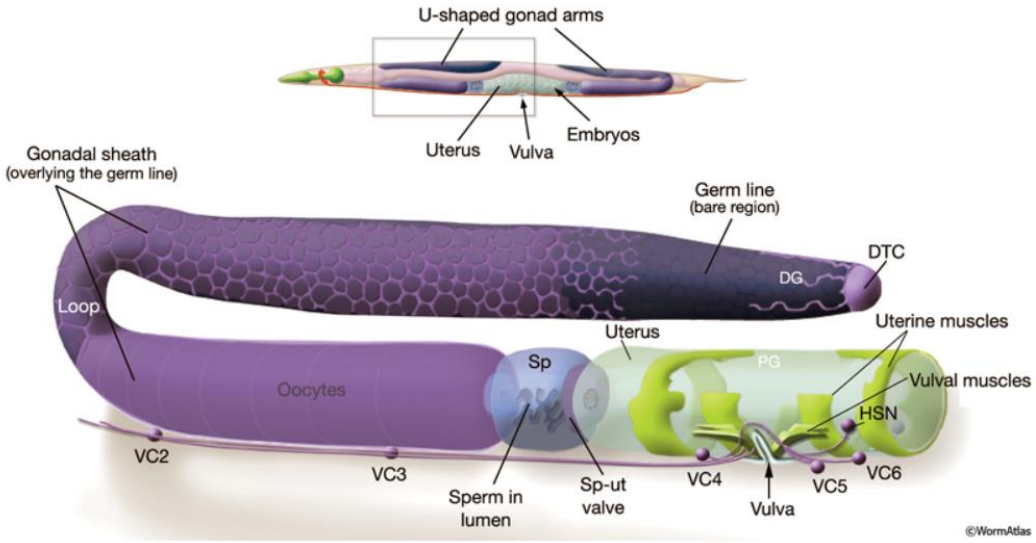

Figure 2 Adult hermaphrodite, lateral view, left side, showing the location of the reproductive system within an intact animal. The reproductive system has twofold symmetry and consists of two U-shaped gonad arms joined to a common uterus. The reproductive system opens to the environment via the vulva,

located in the ventral midbody. (Bottom) One half of the reproductive system, enlarged and separated from other body parts. (DTC) Distal tip cell; (DG) distal gonad; (PG) proximal gonad; (Sp) spermatheca; (Sp-ut) spermathecal-uterine valve (In WormAtlas. doi:10.3908/wormatlas.1.21)

Males in *C. elegans* occur infrequently, appearing at a rate of just 0.1%. They only bear one copy of the X chromosome (XO) and are solely dedicated to producing sperm. [4] Unlike hermaphrodites, males do not produce oocytes and rely on finding potential mates for reproduction. The male reproductive system is geared towards the production and transfer of sperm to hermaphrodites during mating.

Oocytes undergo fertilization as they traverse the spermatheca, a specialized compartment where sperm cells are stored. Following fertilization, embryos move to the uterus, where they develop up to the 30-cell stage. Subsequently, they are expelled as eggs into the external milieu via the vulva. [14,15] The rate of egg-laying varies according to age of the nematode. As documented in existing literature, egg-laying commences approximately 60 hours (~2.5 days) post-egg stage when maintained at 20°C, peaks around 90 hours and then diminishes, ceasing entirely by 120 hours. [6,14,15,17]

4.1.3. Life Cycle

The life cycle of *C. elegans* starts with embryogenesis. Following fertilization, the egg undergoes a series of cell divisions, leading to the emergence of a larva. Subsequent to egg hatching, the organism progresses through four distinct larval stages, designated as L1 to L4. Each of these stages is demarcated by a molt, a process which involves the worm discarding its cuticle during development. [2,4] In response to adverse environmental conditions, such as scarcity of food or overcrowding of population, *C. elegans* is triggered to enter an alternative developmental stage known as the dauer stage (L3 phase). During this stage, worms are conserving their resources, while simultaneously being highly resistant to stress factors. Upon the amelioration of environmental conditions, dauer larvae revert to their developmental trajectory, transitioning to the L4 stage. [6,18] Upon reaching the end of the L4 stage, nematodes attain adulthood. *(Figure 3)* As adults, these nematodes are fecund, with the capability to produce progeny. The lifespan of *C. elegans*, under standard laboratory conditions, lasts approximately 3 weeks. However, it's worth noting that both environmental and genetic factors can influence this duration. [2,4,6]

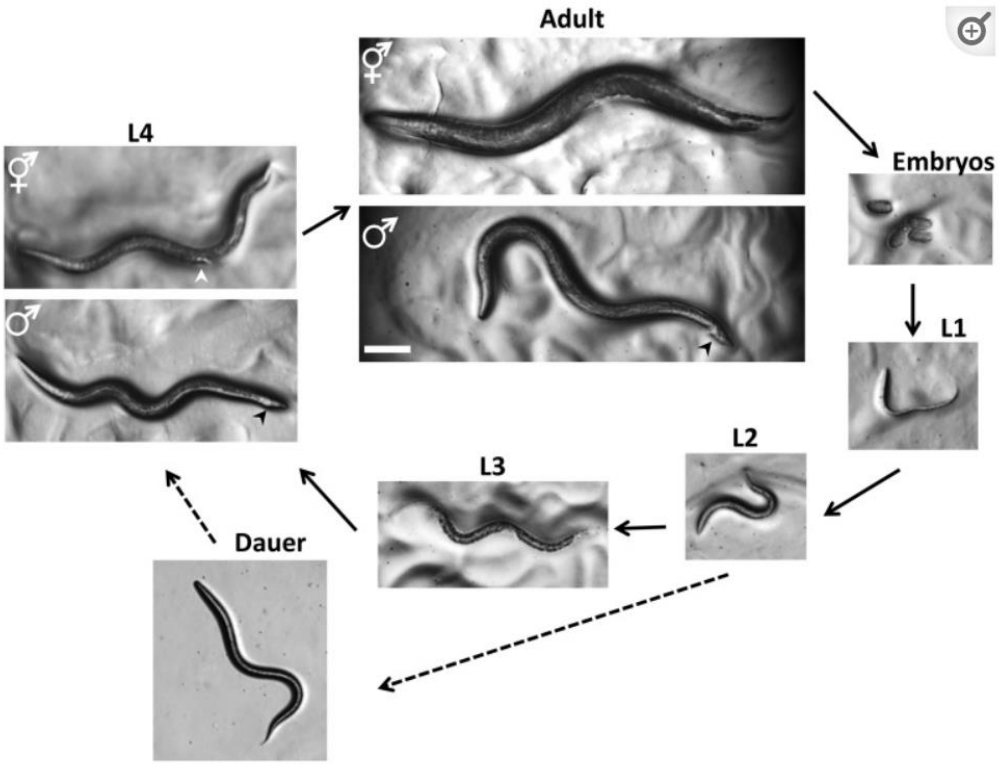

Figure 3 Life cycle stages in *C. elegans*. The eggs, the four larval stages, the dauer stage, as well as the adult animals (hermaphrodite and male) are distinguished. (Source: Corsi et al., 2015)

4.1.4. *Caenorhabditis elegans* as a valuable tool in biological research, epigenetic and metabolic studies

In recent years, *C. elegans* has emerged as a crucial model organism in the study of diverse scientific fields, such as neurobiology, developmental, chemical and molecular biology, as well as medicine for the understanding of various human diseases. [6,19,20] Its facilitated manipulation in biological research is attributed to several distinctive characteristics.

First of all, the nematode's ease of breeding and low-cost of maintenance in laboratory settings provide a robust foundation for exploring intricate *in vivo* biological processes. This is further complemented by its transparent anatomy, making real-time observations of cellular events feasible. [3,4,6] In terms of genetics, *C. elegans* has a well-defined genetic background, as its relatively low complexity allowed for genetic mapping and complete genome sequencing. Additionally, the worm's genome bears a significant degree of similarity to that of humans, since it possesses orthologues for about 40% of the genes responsible for human diseases. Notably, the significance of *C. elegans* as a model system is highlighted by the fact

that many of its molecular pathways are analogous to those in higher species, including humans. [3,4,20]

In the field of metabolic studies, the global rise in metabolic disorders, such as obesity and its associated health risks, have urged for a profound understanding of the molecular pathways governing fat storage and lipid metabolism. *C. elegans* has been instrumental in this regard, because it showcases similarities to mammalian fundamental signaling pathways regarding fat accumulation and processing. Both genetic and environmental factors, influence fat storage in *C. elegans*, thus providing a holistic view of the complex interplay between metabolism and gene regulation. [21]

4.2. Chromatin organization and dynamics

4.2.1. Basic chromatin structure: DNA, histones and nucleosomes

The eukaryotic nucleus serves as a repository of genetic information encoded in DNA. DNA molecules within our cells are not found as lengthy threads in an amorphous state. Instead, they are organized and packaged into a dynamic structure known as chromatin. Genome compaction does not only ensure its efficient protection from external physical and chemical damage, but also plays a crucial role in regulating gene expression, assisting the precision of DNA replication, and orchestrating several DNA repair mechanisms. [22,23]

Chromatin is an intricate and dynamic structure composed of DNA and proteins, also known as histones, that condense to form chromosomes. Histones are alkaline proteins that assemble into an octameric complex, around which DNA is wrapped to form nucleosomes. *(Figure 4)* There are five distinct categories of histones: H1, H2A, H2B, H3, and H4. The histone octamer complex consists of two copies each of the four core histones: H2A, H2B, H3, and H4. These histones interact together so as to form a joint disc-shaped structure, where approximately 147 base pairs of DNA are wound in almost two superhelical turns. For the purpose of chromatin stabilization and support of higher-order chromatin organization, we encounter the linker histone H1, whose function is to link to the DNA as it enters and departs the nucleosome. [24,25] Importantly, the nucleosome comprises the basic repeating unit of chromatin.

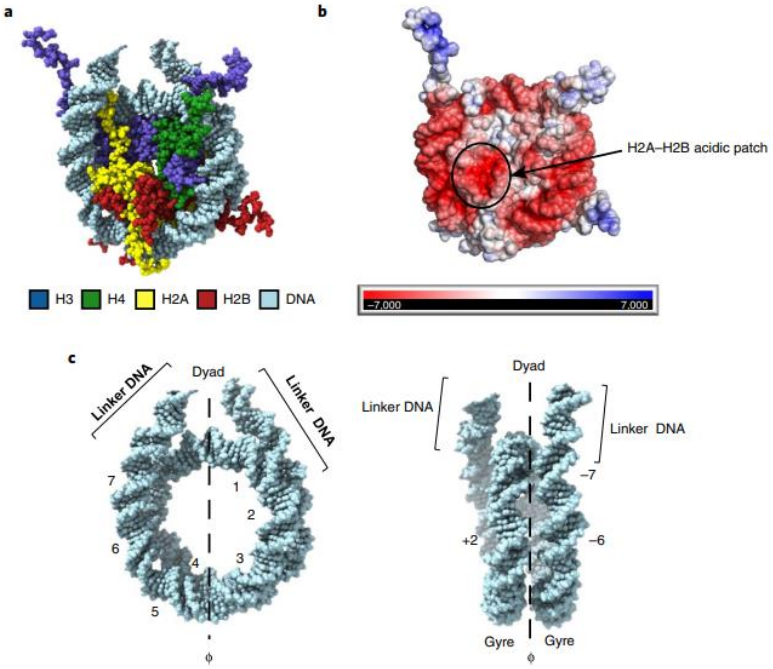

Figure 4. Nucleosome structure. a, Nucleosome disc view (histone octamer) and DNA. b, Electrostatic potential of the nucleosome surface. c, Nucleosomal DNA and linker DNA. Nucleosomal DNA (145–147 bp) can be divided into two gyres (approximately 72 bp each). Linker DNA is the extranucleosomal DNA, which is located next to the entry–exit site of nucleosomal DNA. (Source: Zhou et al., 2018)

Histones are highly conserved proteins in higher organisms *(Figure 5)*, underscoring their fundamental importance in DNA organization and regulation of gene expression. Firstly, their homology among eukaryotic species, including *Homo sapiens* and *Caenorhabditis elegans*, does not only refer to their amino acid sequences but also to their tertiary structures and functions. Secondly, these proteins are prone to diverse post-translational modifications, influencing cellular processes. Their conservation allows for their study in a variety of organisms, shedding light on universal epigenetic mechanisms, as discussed below. [25–27] Tight wrapping of the DNA is made possible because of intense hydrogen bonds paired with electrostatic forces during the interaction of the positively charged histone proteins with the negatively charged nucleic acid. The phosphate backbones of the double helix are brought closer together by the bent conformation of DNA, which is kept in place by the positively charged side chains of the amino acid residues lysine and arginine, therefore neutralizing the negative charges. [28,29]

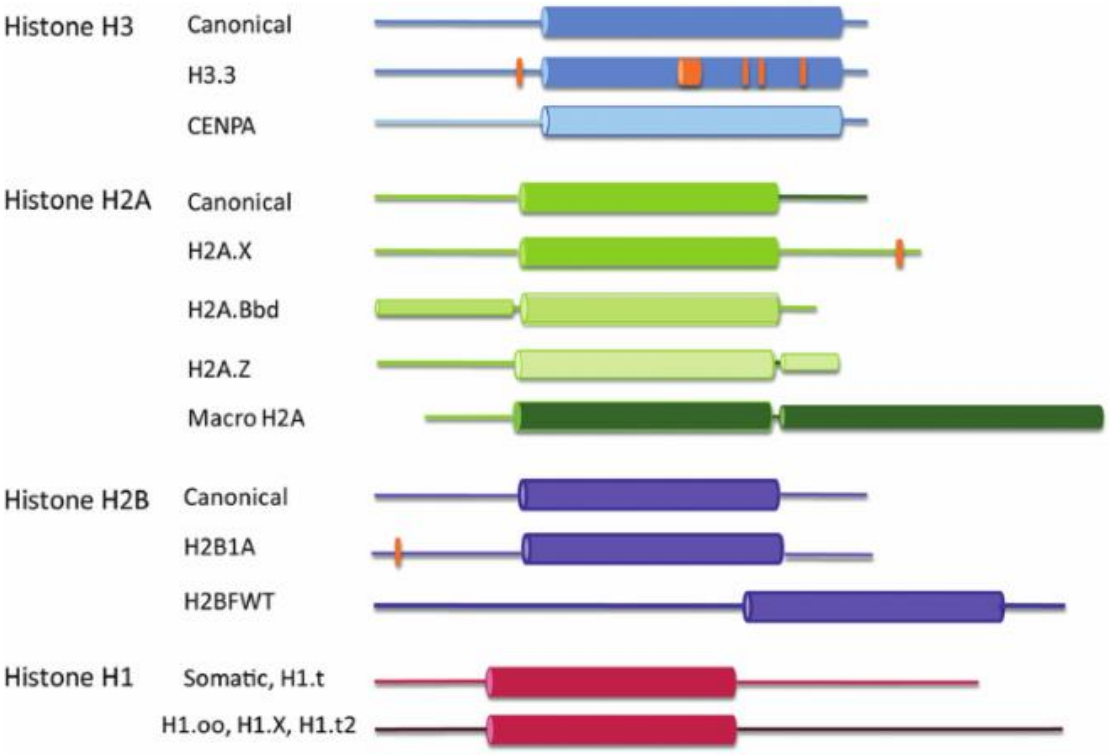

Figure 5 The above shown histone variants contain a highly conserved histone fold domain and vary mainly in their C- and N-terminal sequences. Figure depicts a schematic comparing histone variant sequences. Boxes represent the histone fold domain and orange lines represent site-specific sequence variations. Histones that are in different shades of the same color are from the same histone family but have large differences in sequence. (Source: Liu et al., 2018)

4.2.2. Principles of static and dynamic DNA packaging

As mentioned above, DNA undergoes a multi-level packaging process that involves the compaction of DNA several thousand fold times, with the aid of histones and/or non-histone proteins, thus ensuring efficient storage and functionality. Depending on the stage of the cell cycle, chromatin can be encountered in different structural forms, ranging from a relaxed and diffuse state to a highly condensed and organized configuration. This is achieved by certain histone-modifying enzymes, whose activity fluctuates in a cell-cycle dependent way. [30] Following nucleosome formation, we encounter the primary DNA compaction level in eukaryotic cells, the 10nm fiber. In this configuration, also known as the 'beads-on-a-string' structure due to their distinctive appearance in electron micrographs, nucleosomes are separated by linker DNA segments, ranging from 10 to 60 base pairs in length.

The transition from the 10 nm fiber to the 30 nm fiber is executed by the linker histone, H1, that further recoils linker DNA. There is still uncertainty among the scientific community about the exact model of this configuration, however it is implicitly believed to maintain either a solenoid structure, meaning a single continuous helix, or a 'helical ribbon', where two strands of chromatin fiber are wound around one another. These come as a result of internucleosomal interactions, which are directly dependent on the length variability of the linker DNA, as long as the presence of other chromatin-associated proteins. [31] This structure adopts a helical arrangement of nucleosomes, with six nucleosomes per turn in some models. Contrary to the 10nm fiber chromatin configuration, which is observed to be more transcriptionally active, the 30nm fiber remains repressive *(Figure 6)*. [32]

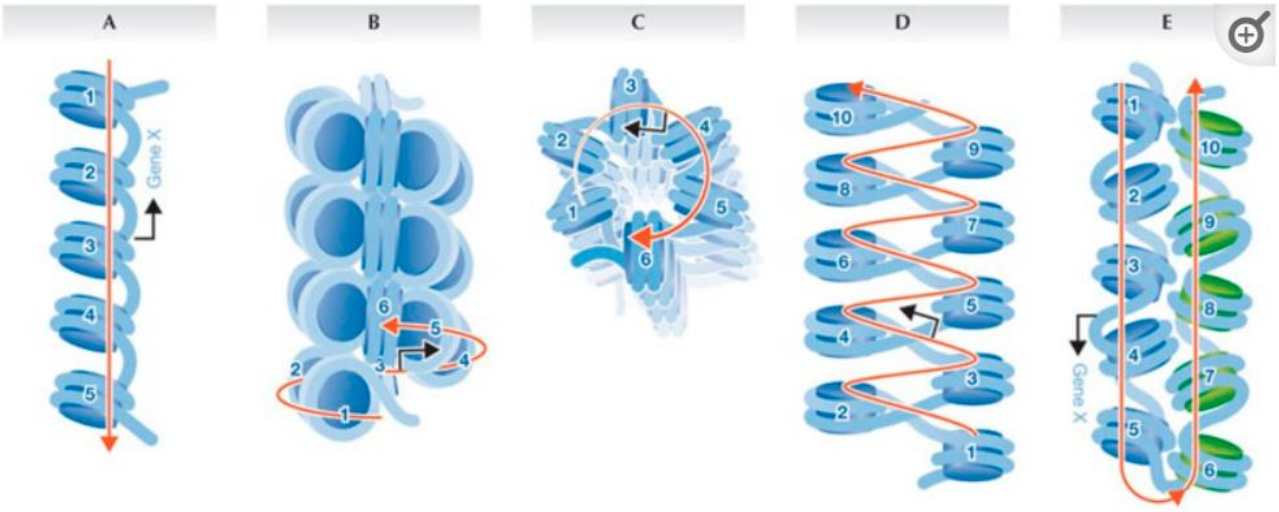

Figure 6 Models of chromatin organization. (A) 10 nm fibre. (B) Side-view of a 30 nm fibre or solenoid. (C) Top-down view of the solenoid. (D) Zig-zag model of the 30 nm fibre. (E) Interdigitation of two 10 nm fibres

(blue against green) forming a boustrophedon. Numbered circles are nucleosomes in an array; red arrow follows the path of the DNA; blue arrow represents a gene promoter. (Source: Quénet et al., 2012)

Beyond the 30 nm fiber, chromatin is subjected to additional compaction, adopting higher-order structures which are important for both transcriptional regulation and the segregation of chromosomes by the mitotic spindle during cell division. The nuclear matrix is thought to provide attachment points for chromosomal DNA. Chromatin loops, which may be tens to hundreds of Kbp long, are formed as an initial step for the achievement of a higher-order structure. These loops are supported at their bases by scaffold or matrix attachment regions (SARs or MARs) to a nuclear matrix or scaffold. S/MARs are 100-1000 bp long AT-rich regions on the genome. They work by bringing distant regulatory components into close proximity with their target genes, contributing to the overall regulation of gene expression *(Figure 7)*. The formation of chromatin loops has also been verified from chromatin immunoprecipitation (ChIP) assays. [33] [34]

Similar to chromatin loops, we encounter other chromatin domains, which are characterized by specific histone modifications and bound proteins. Topologically Associated Domains (TADs) are a noteworthy example of genomic regions, where DNA sequences within them have a higher probability to interact with each other than with sequences outside the TAD. Proteins like CTCF and cohesins make this interaction possible. TADs usually neutralize the action of enhancers to genes within the same domain. [35] [34]

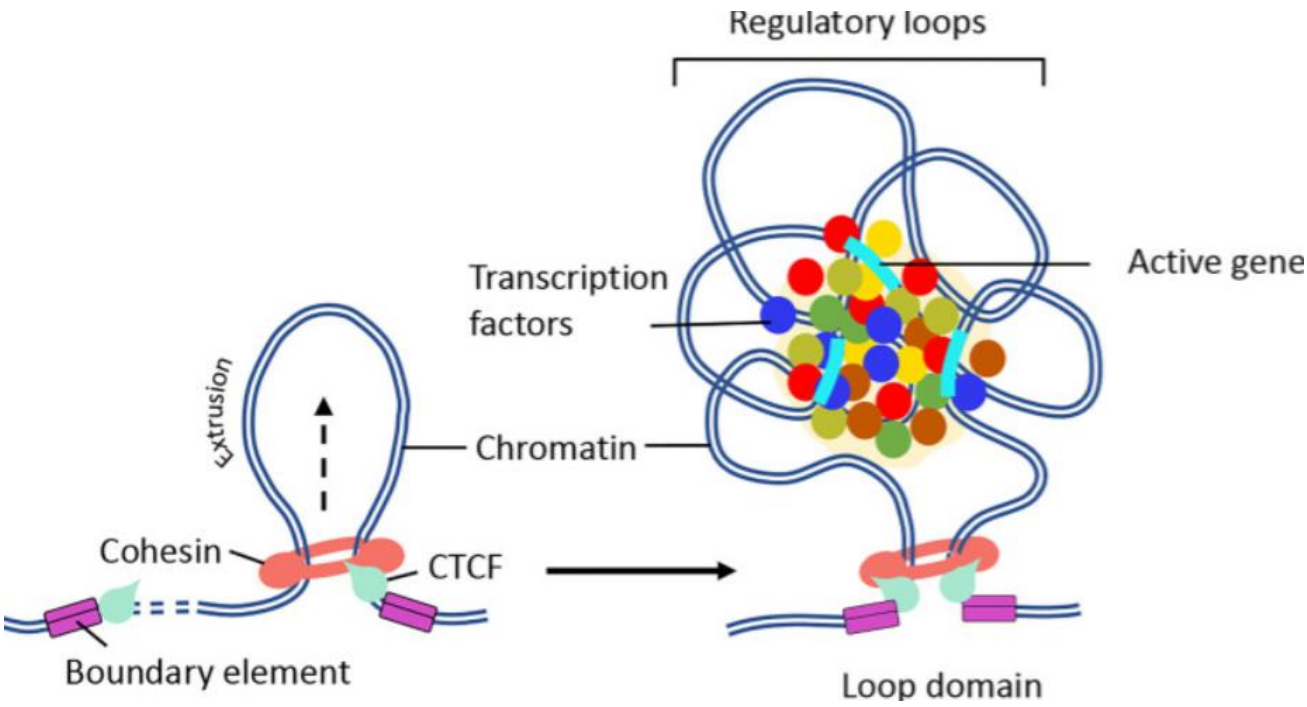

Figure 7 Mechanism of chromatin loop formation. TADs contain varying number of chromatin loops generated through loop extrusion by CTCF/cohesin complexes. Chromatin loop formation facilitates interactions between promoter and enhancer elements. (Right panel) In the presence of NIPBL and MAU2, the cohesin complex loaded on to the DNA. Then, cohesin extrudes chromatin until a pair of convergent CTCF binding sites is reached. (Right panel) The N-terminus of CTCF and convergent positioning of the CTCF-DNA complex stabilizes cohesin binding and stall chromatin extrusion leading to the establishment higher-order chromatin

organization. The intervening DNA between two convergent CTCF sites leads to the formation of a loop domain, which adopts variety of complex shapes comprised of multiple regulatory loops. The internal structure of loop domain is likely determined by polymer chromatin-chromatin self-interactions, which may be further stabilized by phase separation. The contacts within the loop domains facilitate the targeting of enhancers to specific genes. The black arrow depicts the direction of loop extrusion. (Source: Pongubala et al., 2021)

At an even higher level of organization, each individual chromosome occupies distinct regions within the nucleus known as chromosome territories. These territories prevent chromosomes from becoming entangled with one another and may also play a role in regulating gene expression by positioning certain genes at the periphery or center of the nucleus based on their activity

Inside the nondividing nucleus, individual chromosomes occupy specific regions known as chromosome territories. These territories do not only interfere with chromosome entanglement, but also influence gene expression based on their peripheral or central positioning. [36] Even though chromosomes are considered to be static, the relative positioning of territories is not retained after cell division, as different patterns are observed in the nuclei of daughter cells. [37] When the cell enters mitosis, especially during metaphase, chromosomes undergo an intense transformation, by condensing to maximum degree. [38] As expected, during this maximal recoil, chromatin is inaccessible to the cell's transcriptional machinery.

Lastly, we also identify two structural and functional units of chromatin organization, euchromatin and heterochromatin *(Figure 8)*. Euchromatin usually refers to the transcriptionally active part of chromatin, due to its relaxed configuration that facilitates accessibility to transcription regulating elements. Euchromatin is typically located in the inner parts of the nucleus and contains the majority of the active genes. On the other hand, heterochromatin is a highly condensed region, characterized by transcriptional inactivity due to absence of ORFs (although that is not always the case). [39–41]

The primary regions of constitutive heterochromatin formation are pericentromeric and telomeric areas of chromosomes, containing a number of repeating DNA elements, such as transposons and satellite sequence clusters and a vast percentage of the Y human chromosome. Constitutive heterochromatin is continuously present in all cell types and developmental stages, ensuring chromosome stability. Facultative heterochromatin, although not a permanent feature, it is occasionally observed in some cells. It includes genes that are 'dormant' depending on the cell type or the stage of the cell cycle. When these genes are inactive, their DNA regions are compacted into heterochromatin. [42–44]

Euchromatin and heterochromatin display different methylation and acetylation patterns for the regulation of gene expression *(Figure 9)*.

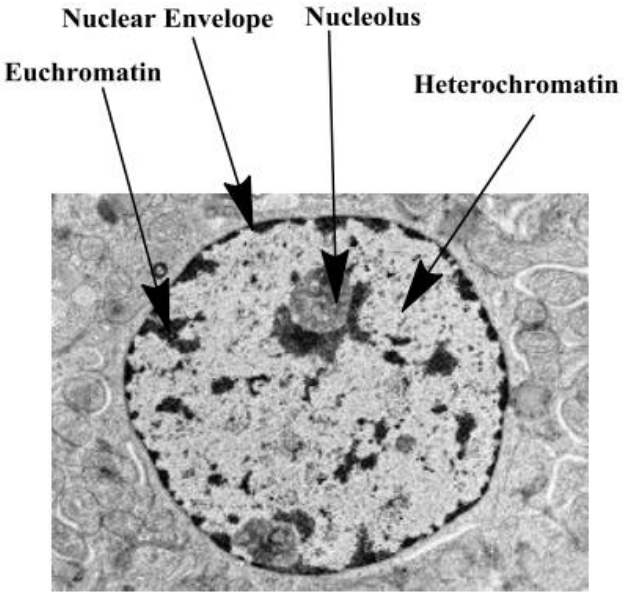

Figure 8 Euchromatin and Heterochromatin within a cell nucleus (Source: Fazary et al., 2017)

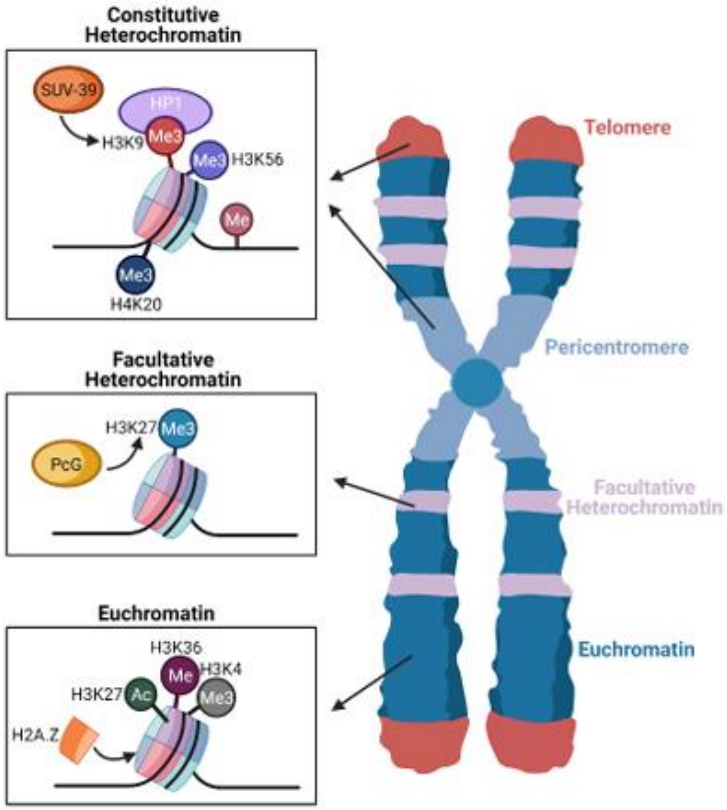

Figure 9 Histone Marks Characteristic of Euchromatin and Heterochromatin. Euchromatin localizes to the chromosome arms and is enriched for the H3K27ac, H3K36me and H3K4me3 histone marks. Additionally, the histone variant H2A.Z can be found in euchromatic nucleosomes. Constitutive heterochromatin is observed at the subtelomeric and pericentromeric regions of chromosomes. Histone marks typical of constitutive heterochromatin include H4K20me3, H3K56me3 and H3K9me2/3, of which the latter is deposited by the

methyltransferase SUV-39 and associates with the heterochromatic protein HP1. DNA packaged into constitutive heterochromatin is enriched for methyl groups. Facultative heterochromatin is distributed along the chromosome arms and is characterized by the presence of the histone mark H3K27me3, deposited by the proteins of the Polycomb group (PcG). This figure was created on Biorender.com. (Source: chrome-extension://efaidnbmnnnibpcajpcglclefindmkaj/https://studenttheses.uu.nl/bitstream/handle/20.500.12932/389/Writing_Assignment_Arianna_Sandron.pdf?sequence=1&isAllowed=y)

The principles of DNA packaging and chromatin organization are vastly conserved in the nematode *C. elegans*, making the study of gene regulation simpler and more uncomplicated.

4.2.3. Role of chromatin structures in gene regulation and expression

Chromatin structures and organization patterns described above provide the necessary conditions for efficient genome compaction and the subsequent regulation of gene expression in eukaryotic cells. [45] Different levels of DNA density, as encountered in euchromatin and heterochromatin configurations, can either grant access to the transcriptional machinery of the cell or act as a barrier, thereby silencing gene expression. [39] Genome expression can be influenced in terms of nucleosome and DNA modifications.

Chromatin remodeling is a dynamic process that modulates nucleosome repositioning through the aid of ATP-dependent remodeling protein complexes. Nucleosome repositioning refers to the nucleosome movement alongside the DNA strand. In that case, binding of transcription factors can be regulated. Examples of nucleosome repositioning include nucleosome sliding, nucleosome eviction, or histone exchange. [46] Moreover, post-translational modifications of histone targets, such as acetylation, methylation, phosphorylation and ubiquitination can modify chromatin structure and its degree of accessibility. All of these chemical alterations constitute epigenetic markers, which direct the recruitment of certain proteins that can either promote or repress transcription. [47]

Fundamentally, the control of gene expression is orchestrated by the dynamic nature of chromatin structures, which alternate between open and closed conformations. This guarantees that the proper genes are expressed in the right cells at the right timeframes. For the purpose of our study, we will delve deeper into some of the main epigenetic markers on *C. elegans*, that dictate gene regulation of immense cellular metabolic processes.

4.3. Epigenetic modifications

4.3.1. Definition and significance of epigenetics

The history of epigenetics is intertwined with that of evolution and developmental biology. However, during the past 50 years, the definition of the term "epigenetics" has evolved, keeping pace with our greatly increased understanding of the molecular mechanisms controlling the expression of genes in eukaryotes. Our current definition of epigenetics is a reflection of what we now know and comprehend about it. [48]

Epigenetics is the study of molecular mechanisms by which heritable traits can be passed down to descendants, without any alterations occurring in the nucleotide sequence of DNA. These traits are associated with chemical modifications of the DNA or the core histone proteins attached to it and are called 'epigenetic markers'. [49,50] Epigenetic markers are not removed by cell division and can vastly affect the cell's gene expression. [51,52] They either occur as part of normal development or as a response to various environmental factors, dictating cellular and physiological phenotypic traits. [53]

Some of the primary epigenetic modifications include DNA methylation, histone modifications, RNA interference, chromatin remodeling, genomic imprinting and X-chromosome inactivation. In this study, we are mostly going to focus on epigenetic modifications of histone and non-histone targets.

The study of epigenetics is of great biological and medical importance, because it has made revolutionary contributions to our knowledge of heredity and gene expression. Epigenetics emphasize that gene expression patterns may be altered by environmental stresses, resulting to a variety of phenotypes without changing the DNA sequence, contrary to the conventional assumptions that genes control our fate. These epigenetic changes may have long-lasting effects, affecting cognitive functions, as well as predispositions to certain malignancies. Epigenetic marks that are incorrect or abnormal can cause birth defects, childhood illnesses, and disease symptoms at different stages of life. [51] Additionally, epigenetic modifications have been linked to a plethora of illnesses, including but not limited to cancer, metabolic disorders, neurological conditions, and cardiovascular diseases. Researchers are searching for new therapeutic approaches, including drug designing targeting epigenetic marks, in an attempt to take advantage of their potential reversibility. Such interventions are very promising as possible therapies for a variety of disorders, underscoring their enormous significance in influencing the future of medicine. [51,52]

4.3.2. Epigenetic modifications of histone proteins

Histone proteins can undergo a number of post-translational modifications, including acetylation, methylation, phosphorylation, ubiquitination, citrullination to name a few. Acetylation and methylation are among the most prominent histone modifications in terms of transcriptional regulation. [54]

Histone acetylation involves the reversible covalent addition of an acetyl group (-Ac) to the ε-amino group of lysine residues on the N-terminal histone tails projecting out of the nucleosomes. The enzymes involved in this process are called Histone acetyltransferases (HATs), while Histone deacetylases (HDACs) reverse the addition of acetyl groups *(Figure 10)*. Acetylation of H3 and H4 histone proteins is usually associated with increased transcriptional activity.[55] Acetyl groups counteract the positive charge of histone lysine residues, thereby weakening the electrostatic affinity between histones and negatively charged DNA *(Figure 11)*. This leads to chromatin adopting a more relaxed configuration, allowing accessibility to transcriptional elements. However, histone deacetylation represses active regions of the genome. [45,56]

All histone proteins can be acetylated in various lysine residues. Specific acetylation patterns and combinations vary depending on the cellular context, and the presence or absence of specific acetylation marks can have different functional implications for gene expression and chromatin structure. For example, chromatin structure is influenced by H4K16 deacetylation and H4K12 hypoacetylation combined with H3K56 hyperacetylation, which collectively create a chromatin environment conducive for the transcription of constitutive genes. This research found that the expression of active genes was higher in H4K16R mutant, which mimics the deacetylated state, as opposed to H4K16Q which mimics constitutive acetylation. This suggests that specific histone modifications, especially around lysine residues, directly influence gene transcription. [43]

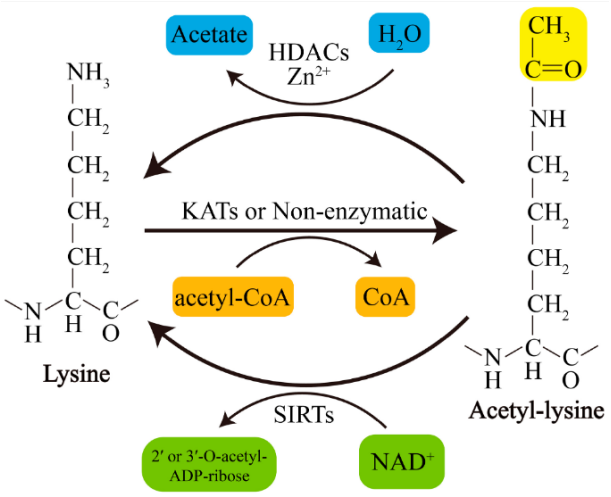

Figure 10 Schematic overview of lysine acetylation and deacetylation. Lysine acetylation, which is catalyzed by KATs, involves transfer of an acetyl group from Ac-CoA to the ε-amino side chain of lysine or occurs nonenzymatically. Deacetylation of lysine residues is catalyzed by Zn2+-dependent HDACs or by NAD+-dependent SIRTs. NAD+, nicotinamide adenine dinucleotide. (Source: Wang et al., 2020)

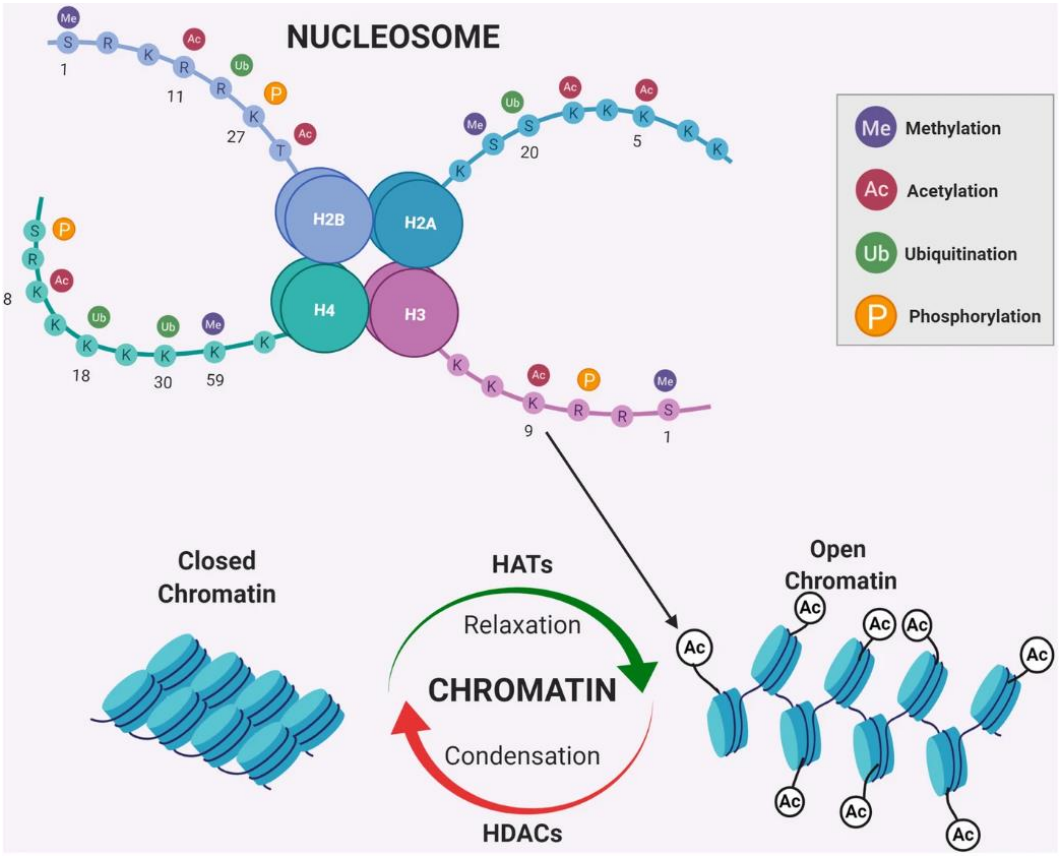

Figure 11 Histone acetylation. Protruding histone tails undergo post translational modifications such as methylation, acetylation, ubiquitination and phosphorylation. The numbers indicate the positions of targeted lysine groups. Histone acetylation alters the conformation of chromatin structure in nucleus by relaxing the chromatin and allowing transcriptional activation. It is regulated by two sets of enzymes HATs and HDACs which add or remove acetyl group respectively from both histone and non-histone proteins, hence regulating gene transcription. (Source: Gujral et al.,2020)

Histone methylation is also a post-translational modification that plays a pivotal role in regulating gene expression and it involves the covalent addition of methyl groups (-Me) leading to mono-, di-, or tri-methylated basic amino acid residues, like lysine or arginine. Methylation is carried out by specific enzymes called Histone methyltransferases (HMTs) and can be reversed with Histone demethylases (HDMs). Unlike acetylation, histone methylation does not alter the electrostatic affinity of DNA bound to histones, rather than marks specific amino acid residues with a varied number of methyl groups. The term "histone code" suggests that the presence of a methyl group close to a lysine residue can influence the addition or removal of an acetyl group on a neighboring lysine residue, thereby integrating multiple downstream signaling pathways and coordinating the cellular response *(Figure 12)*.

[57,58] Depending on the methylation pattern, gene transcription can either be enhanced or suppressed *(Figure 13)*. [54,59]

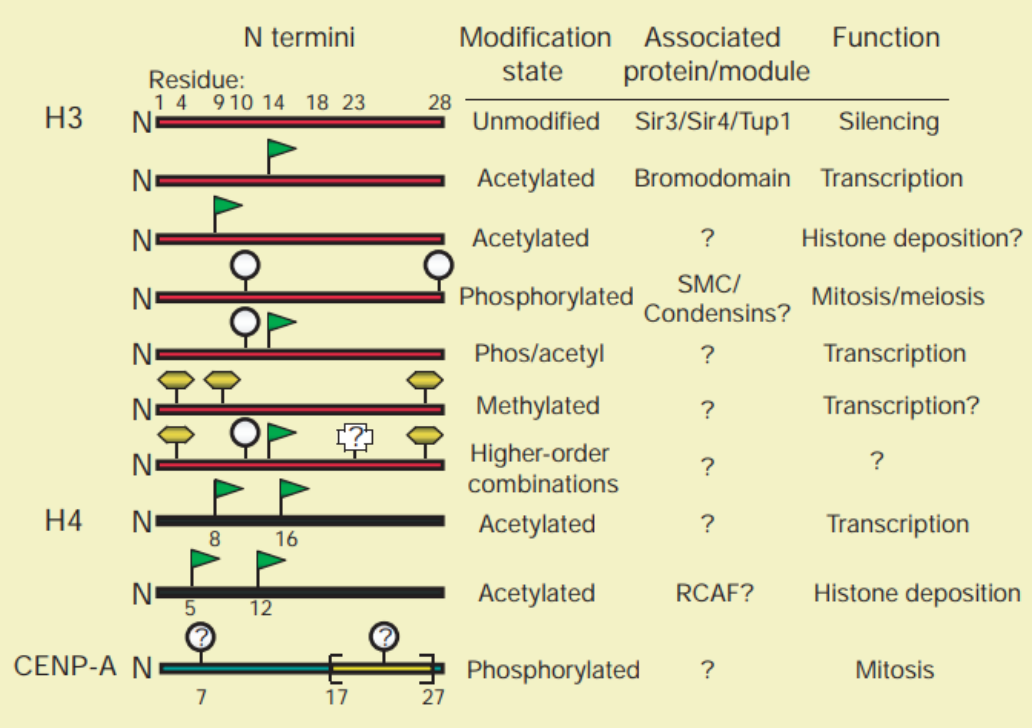

Figure 12 The `histone code' hypothesis. Histone modifications occur at selected residues and some of the patterns shown have been closely linked to a biological event (for example, acetylation and transcription). Emerging evidence suggests that distinct H3 (red) and H4 (black) tail modifications act sequentially or in combination to regulate unique biological outcomes. How this hierarchy of multiple modi®cations extends (depicted as `higher-order combinations') or how distinct combinatorial sets are established or maintained in localized regions of the chromatin fibre is not known. Relevant proteins or protein domains that are known to interact or associate with distinct modifications are indicated. The CENP-A tail domain (blue) might also be subjected to mitosis-related marks such as phosphorylation; the yellow bracket depicts a motif in which serines and threonines alternate with proline residues. (Source: Strahl and Allis, 2000)

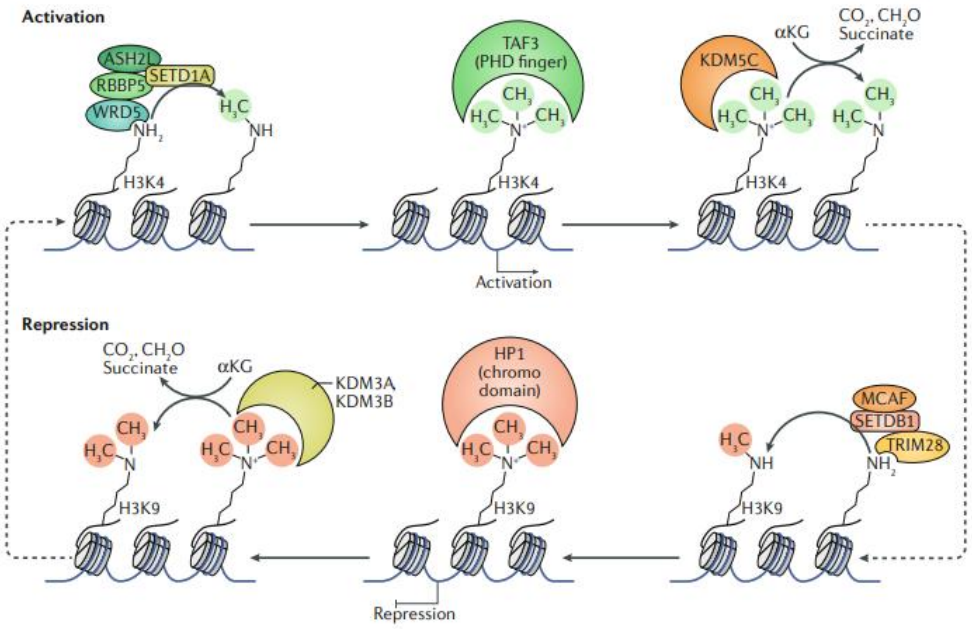

Figure 13 Examples of regulation of gene expression by histone methyltransferases and demethylases. SETD1A methyltransferase complex (comprising SETD1A (a catalytic SET-domain subunit), together with the binding partners ASH2L, RBBP5, WDR5 and other complex-specific subunits not shown) deposits the gene-activating H3 Lys4 tri-methyl (H3K4me3) mark at the promoters of various genes. H3K4me3 is recognized by PHD finger domains in proteins such as TAF3, which bind to methylated Lys. Gene activation can be reversed through the removal of this modification by the demethylase KDM5C, which utilizes α-ketoglutarate (αKG) as a cofactor. Gene-repressive states can be established by the deposition of H3K9me3 by the SETDB1 histone methyltransferase complex (including the catalytic subunit SETDB1 together with a regulator, MCAF (also known as ATF7IP) and a reader protein, TRIM28). H3K9me3 is recognized by the chromodomain in HP1 proteins and can be removed by the KDM3A and/or KDM3B demethylase in the presence of αKG as a cofactor, to allow for gene activation. (Source: Jambhekar et al., 2019)

For example, trimethylation of histone H3 at lysine 4 (H3K4me3) is often found near transcription start points and is associated with gene activation. In contrast, trimethylation of histone H3 at lysine 27 (H3K27me3) is linked to gene repression. [43] In *C. elegans*, histone H3K4 trimethylation (H3K4me3) plays a key role in the transgenerational inheritance of obesogenic effects by marking genes related to lipid metabolism and upregulating their transcription. Thus, the effects of lipid accumulation from a high-fat diet treatment can be epigenetically transmitted to multiple generations. [60]

Despite the fact that methylation patterns can be stable through meiosis, mitosis, and even inheritance, their dynamic nature allows them to contribute to phenotypic variety. Diseases like cancer and intellectual impairments can result from disturbances in this methylation equilibrium. Histone methylation levels change in accordance to age and are involved in many biological processes, including DNA repair, transcription, and ageing. Methylation regulating enzymes have the potential to affect lifespan and exhibit transgenerational effects. [59]

4.3.3. Epigenetic modifications of non-histone proteins

For the most part, the majority of research concerning epigenetic regulations has focused on chemical modifications to core nucleosome histone proteins. However, attention has shifted towards elucidating mechanisms of epigenetic modifications on non-histone targets, which are of great biological importance.

Non-histone epigenetic modifications do not only refer to DNA methylation or RNA (lncRNA, siRNA) modifications, but also to a steadily growing number of proteins who have been identified as targets, including transcription factors, tumor suppressor proteins, hormone receptors, chaperones or other signaling pathway molecules. These modifications play a crucial role in regulating cellular processes, like gene expression, cell signaling, and cell fate decisions to name a few, thus further accentuating their research significance. [61]

Acetylation of protein targets, beyond histones, is a critical post-translational modification regulating their cellular and molecular activity. Similar to histones, acetyl groups are covalently added to lysine amino acid residues of non-histone proteins, with the aid of HAT enzymes. This leads to alterations in their activity, stability, interactions, and localization. [61] Examples of identified non-histone substrates for acetylation include the transcription factor NF-κB and the tumor suppressor protein p53, whose acetylation state can affect both their DNA-binding ability and their transcriptional activity. [62] Furthermore, the histone acetyltransferase MYST family, which controls gene-specific transcriptional activity, DNA replication, and DNA damage response, also acetylates non-histone proteins linked to Alzheimer's disease. [63] Another study highlighted the role of HDACs in modulating the acetylation levels of non-histone proteins, like HDAC inhibitors *(Figure 14)*. It has been shown that deviant HDAC activity negatively impacts DNA damage response (DDR) in cancer, due to their direct involvement in the acetylation of several DDR proteins. [64] In *C. elegans*, non-histone acetylation targets is still an ongoing field of biological research, with lots of potential in the development therapeutic approaches for neurodegenerative and metabolic disorders.

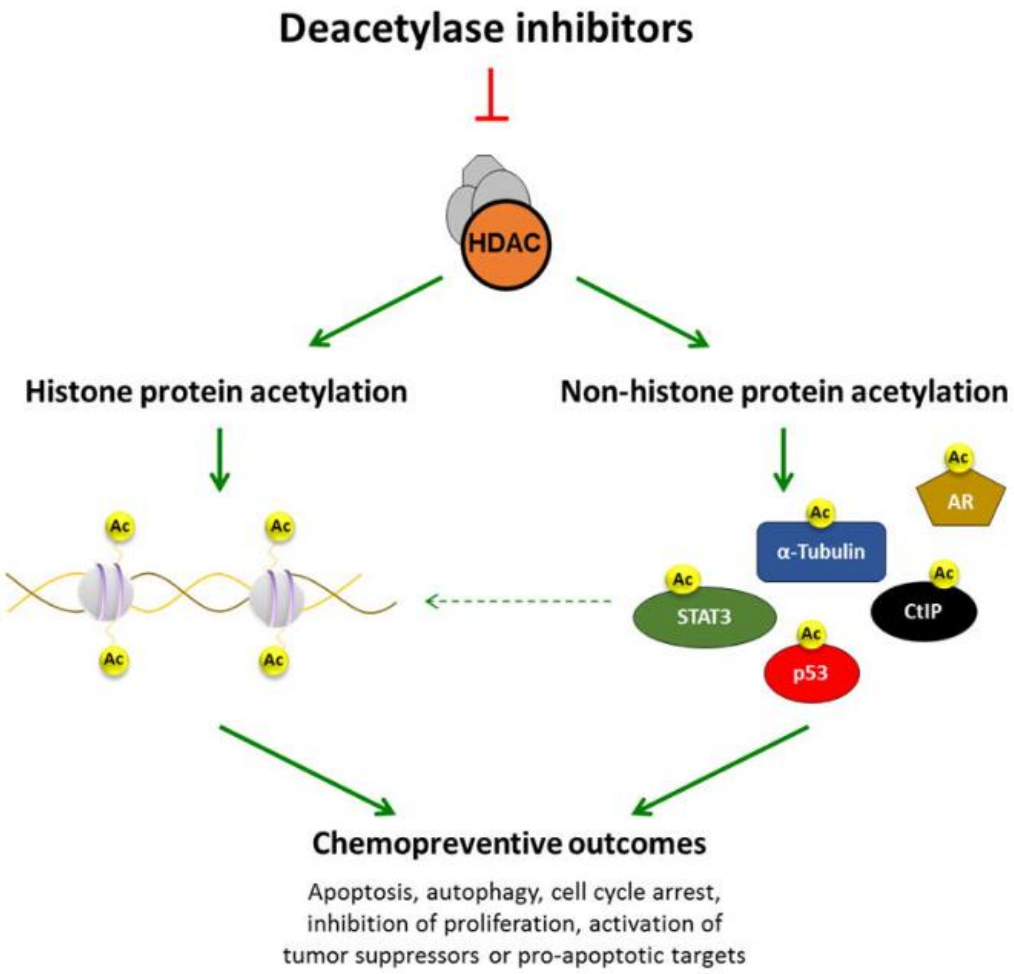

Figure 14 Dietary deacetylase inhibitors and (de)acetylation targets. Deacetylase inhibitors induce histone hyperacetylation leading to an open chromatin conformation that correlates with gene activation. Acetylation of non-histone proteins modulates their function, stability, cellular localization, and/or protein–protein interactions. Transcription factors such as STAT3 and p53 are directly acetylated by HDAC inhibitors, which can positively or negatively alter their capacity to bind DNA and modulate gene expression. Through the combined effects on histone and non-histone protein acetylation, deacetylase inhibitors exert chemopreventive outcomes ranging from inhibition of cell growth, cell cycle arrest, apoptosis, autophagy, or necrosis. (Source: Kim et al., 2016)

Similarly, another post-translational modification that goes beyond the extensively researched area of histone methylation is the methylation of non-histone substrates. Non-histone proteins undergo alterations, that entail the covalent insertion of a methyl group to certain amino acid residues, typically lysine, affecting their function and having an impact on a number of cellular processes. These modifications are made by a vast enzyme family known as protein methyltransferases. Methylation of lysine residues is executed by a specific group of methyltransferases called KMTs. [65] These enzymes modify the target protein's activity, localization, or interaction with other proteins by transferring a methyl group from S-adenosyl methionine (SAM) to it *(Figure 15)*. [66,67]

A well-characterized familiy of methyltransferases is the PRDM family. Enzymes of this family, such as PRDM15, play a role in cellular proliferation, differentiation, and are often deregulated in diseases like cancer. Methyltransferase PRDM15, an uncharacterized transcriptional regulator, could potentially contribute to non-histone methylation, as suggested by *in silico* approaches of their native non-histone substrates. [68] Recent findings have identified a SET domain-containing enzyme, SET7/9, as a key component in the methylation of both histone and non-histone proteins. This proves that lysine methylation is not functionally limited to chromatin remodeling. [69] Moreover, The hypoxia-inducible factor (HIF) pathway is triggered by low oxygen levels and it aids in cell adaptation under acute circumstances. At steady oxygen levels, cellular oxygen sensors inhibit HIF activity, while also influencing G9a and G9a-like protein (GLP), two lysine methyltransferases. These enzymes become more active in hypoxia and have an impact on a number of non-histone proteins, like LaminB1 (LMNB1), stabilizing it and connecting it to the nuclear perimeter. [70] In the context of *C. elegans*, LMNB1 protein homologue is also targeted by euchromatic histone methyltransferases (EHMTs), members of the KMT1 family, whose activity extend beyond histone methylation. A study by Rao et al. demonstrated that EHMTs methylate and stabilize LMNB1, associating it with H3K9me2 peripheral heterochromatin. This methylation is responsible for the anchoring of heterochromatin at the nuclear periphery. The study also highlighted implications of EHMT depletion related to aging and cellular organization. [71] Finally, another study on liver cancer focused on the function of PRMT5, a protein arginine methyltransferase. Through arginine methylation, PRMT5 regulates the interplay between the E3 ubiquitin ligase ITCH and the transcription factor RORα. The stability of RORα and its target genes are impacted by this interaction. Reactive oxygen species (ROS) are also involved, decreasing PRMT5 levels and raising RORα levels, exhibiting a complex interrelationship between ROS, PRMT5, and non-histone methylation in liver cancer. [72]

The aforementioned examples from existing scientific literature showcase the need to combine data from epigenetic modifications of non-histone substrates along with other posttranslational alterations, in order to better understand complex cellular dynamics and disease pathogenesis. [66] The significance of non-histone protein changes in the context of cellular function and illness is becoming more and more clear, as our knowledge of the epigenetic landscape is constantly evolving.

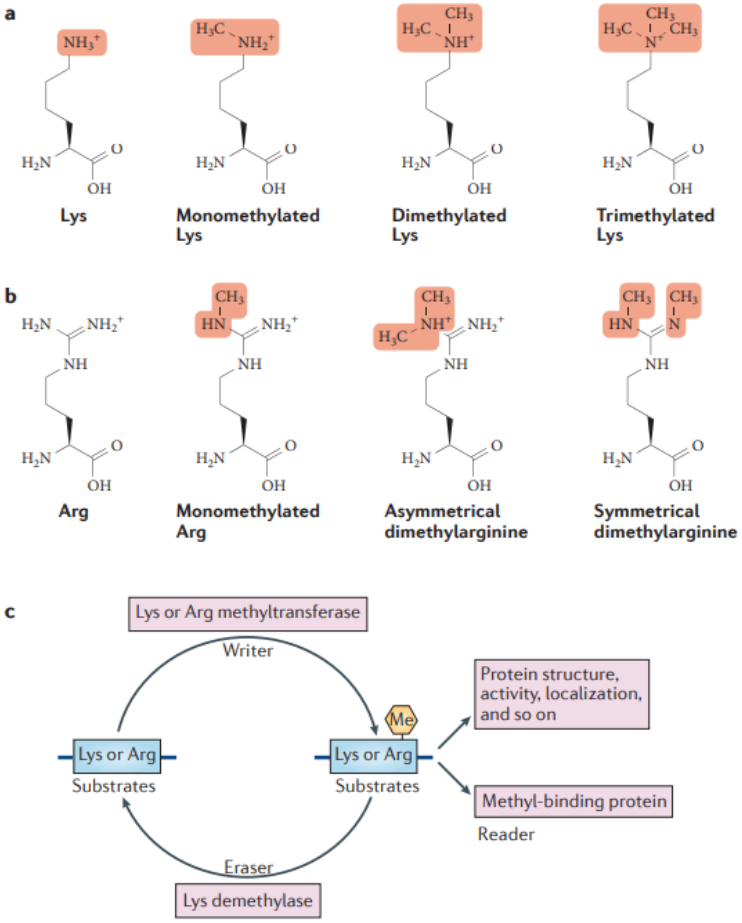

Figure 15 a) A Lys residue can undergo mono-, di- or trimethylation at its side chain ε-amine. b) Although Arg is not able to undergo trimethylation, two distinct forms of dimethylation (asymmetrical and symmetrical) can occur on its side-chain guanidino cation group, in addition to monomethylation. Methyl groups and methylated nitrogen atoms are shown in red. c) Protein methylation is directly comparable to phosphorylation, as the modification can be dynamically added to substrates by writer proteins or removed from them by eraser proteins. Methylation may influence protein structure, activity, subcellular localization, or interactions with reader proteins, which contain a modular domain that can interact with the methylated residue. (Source: Biggar et al., 2015)

4.3.4. SET domain proteins and their role in epigenetic regulation

Within the scope of this thesis research project, our primary focus will be on the subject of SET domain-containing proteins and their role as epigenetic factors.

The SET domain is a conserved sequence motif found in a superfamily of enzymes primarily recognized for their histone methylation activity. This superfamily encompasses almost all proteins known to methylate histones on lysine amino acid residues (HKMTases), thereby regulating gene expression. [73] However, there have been identified other enzymes within this superfamily with a methyltransferase activity towards non-

histone substrates, as in the example of SET7/9 described above *(Figure 16)*. [69] The acronym "SET" derives from three *Drosophila melanogaster* HKMTases where this domain was first discovered: Suppressor of variegation 3-9 [Su(var)3-9], Enhancer of zeste [E(z)], and Trithorax [Trx]. [74,75]

Adjacent to the SET domain, many proteins also contain additional regions known as the pre-SET and post-SET domains. The pre-SET domain is situated in the N-terminal of the enzyme, where one can find the presence of multiple cysteine residues. The zinc-finger-like structure of the domain is due to the coordination of zinc ions by these cysteines, leading to the formation of a triangular Zn_3Cys_9 zinc cluster. The pre-SET domain is instrumental for the stabilization of the protein's SET domain and plays a crucial role in enhancing its methyltransferase activity. [76] The post-SET domain is situated in the C-terminal region, following the SET domain. A zinc-binding site is created by the three conserved cysteines in the post-SET domain and coupled with a fourth conserved cysteine, they form a structure that resembles a knot adjacent to the SET domain active site. The C-terminal residues involved in histone tail interactions and S-adenosyl-L-methionine-binding are brought in by the structured post-SET region. The three conserved cysteine residues are necessary for HMTase function because serine replaces them and renders HMTase inactive. [77]

Human genes encoding proteins containing this domain include SUV39H1 and SUV39H2. These methytransferases di- and trimethylate histone H3 lysine 9 (H3K9), which is important for maintaining heterochromatin and suppressing gene activity. Their active SET domain and chromodomain binds H3K9me2/3, helping in enzyme targeting. Apart from histones, these enzymes also methylate various non-histone proteins, indicating their diverse roles in cellular processes. [78]

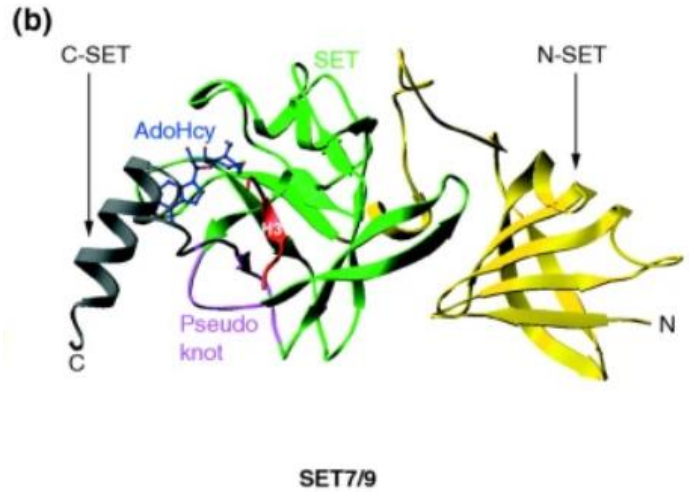

Figure 16 Human SET7/9. The pre-SET, SET, and post-SET domains are indicated. The pseudoknot formed by two conserved SET motifs and the bound histone H3 peptide are also illustrated. Zinc ions are shown as balls. N, amino terminus; C, carboxyl terminus. (Source: Dillon et al., 2005)

For the purpose of our study, we are using five knockout *C. elegans* strains, four of which are mutants for various genes of the *set* superfamily, precisely *set-4*, *set-14*, *set-18* and *set-30*. Based on current scientific literature, a number of *set* genes have been identified and characterized based on their biological role. A notable example is the *set-32* gene, known for its role in establishing the heterochromatin mark H3K23me3 that is remarkably linked to transgenerational epigenetic inheritance, via RNAi-mediated chromatin changes. [79] Also, the *set-2* gene is the *C. elegans* homologue of human H3K4 methyltransferase genes KMT2F/G (SETD1A/B), influencing the transcription of neural genes during embryogenesis. [80] Lastly, the *set-17 C. elegans* gene encodes for a SET domain containing protein like PRDM9 and PRDM7 in humans, which regulates the gene expression of primary spermatocytes, thereby aiding in fertility. [81]

However, there is still much to uncover about the role of *set* genes in the nematode *C. elegans*. Our study endeavors to contribute to further bridging this gap, by elucidating their epigenetic role.

4.4. Dietary influences on gene regulation, healthspan and senescence

4.4.1. Lipid structure and functions

Lipids make up a diverse and ubiquitous group of organic molecules with hydrophobic properties, which depending on their structural and functional characteristics, they can be broadly categorized into triacyglycerols, phospholipids, steroids and waxes. [82] In our study, we are assessing the effects of a high-fat diet (HFD), supplemented with lipids and essential nutrients found in chicken egg yolk. Egg yolk constitutes a rich source of lipids, extending from cholesterol to fatty acids. The lipids within an egg yolk comprise about 33% of its whole weight. [83]

It is noteworthy that egg yolk contains a substantial amount of monounsaturated fatty acids (MUFAs), primarily oleic acid. Monounsaturated fatty acids were found to be far more abundant than saturated fatty acids and polyunsaturated fatty acids in egg yolks. [84] Structurally, MUFAs contain one double covalent bond in their fatty acid chain, as opposed to saturated fatty acids containing no double bonds or polyunsaturated fatty acids containing multiple double bonds. Oleic acid is found in *cis*-configuration, where hydrogen atoms are on the same level as the covalent bond *(Figure 17)*. [85] Fluidity of the cell membranes is partly attributed to this single double bond of MUFAs. Egg yolk MUFAs offer numerous health advantages, such as reducing cholesterol levels and potentially reducing the risk of heart disease. They also serve as energy sources and help in the absorption of fat-soluble vitamins. [86]

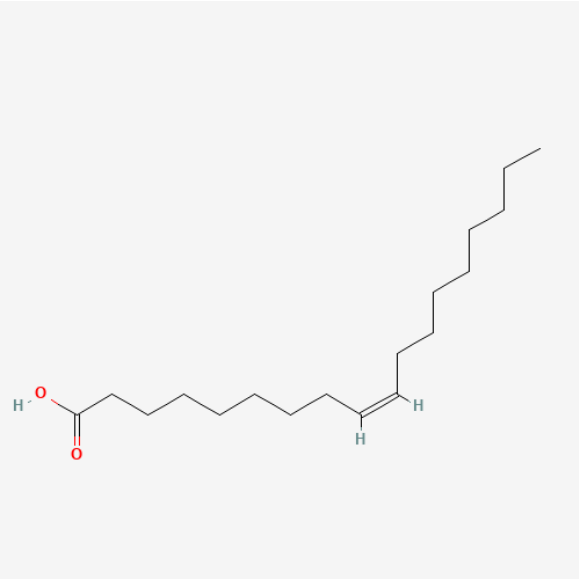

Figure 17 Structure of oleic acid, the most abundant MUFA in egg yolk, in cis-configuration. (Source: PubChem)

Lipids play a multifaceted role in cellular functions, including energy source reservoirs, components of cell membranes and as signaling molecules in a plethora of pathways. [87,88] Normally, through the process of lipolysis, triglycerides are converted to glycerol and fatty acids. These fatty acids are subsequently transported to mitochondria, where they engage in β-oxidation to produce acetyl-CoA. After entering the citric acid cycle, this acetyl-CoA leads to the production of ATP molecules. During this process, electrons are released and transferred to NAD+ and FAD, leading to the formation of the coenzymes NADH and $FADH_2$. Both of these coenzymes are later deployed in oxidative phosphorylation, which in turn promotes ATP generation in mitochondria. [89]

Recent scientific studies have stressed the significance of lipids as signaling molecules that actively influence the epigenome of an organism. [90] Since then, there has been an increase in the number of scientific studies conducted focusing on the impact of obesogenic factors, notably a HFD, on epigenetics and the control of gene expression in various organisms. Dietary habits are known for affecting various physiological processes in the body, rendering their understanding crucial for optimal health and disease prevention. [87,91,92]

4.4.2. The interplay between a high-fat diet and epigenetic modifications

High-fat diets can lead to specific changes in the expression of certain genes due to epigenetic modifications. For instance, genes involved in metabolism, appetite regulation, and energy expenditure can be particularly affected, leading to conditions like obesity, insulin resistance, and other metabolic disorders. The relationship between a lipid diet and the epigenome has been thoroughly elaborated in scientific literature, as stated by the overview provided below.

One of the primary mechanisms that is vastly impacted by a HFD is that of DNA methylation. [91] A study by Vucetic et al. has suggested that a HFD during rodent pregnancy affected the DNA methylation patterns of the offspring's dopamine and opioid-related genes. As a result, particular dietary preferences among the progeny were found to be connected to altered gene expression levels, due to DNA methylation. [93] A similar study in mammals investigates the effect of DNA hydroxymethylation in mice fed with a HFD, that later develop cardiac issues connected to obesity. The research shows that cardiac problems in these animals are correlated with alterations in tissue- specific DNA methylation/hydroxymethylation patterns and associated enzymes. These observations point to a link between certain genes and obesity-related cardiac problems. Deeper understanding of the epigenetic causes of the obesity-related cardiac repercussions may come through further study. [94] Moreover, a study in mice proposes that dietary fat disrupted

pathways related to cytokine interaction, chemokine signaling, and oxidative phosphorylation in mice. [91] Non-alcoholic fatty liver disease (NAFLD), a disorder that is common in Western nations and is frequently associated with diets rich in saturated fats, has been a topic of great research interest concentrated on the epigenetic control of the PPARγ gene in HFD-fed mice and palmitic acid-exposed liver cells. The study demonstrated that a high-fat diet decreases methylation levels in the PPARγ gene promoter, which results in an increase in the production of PPARγ and associated genes and an excessive buildup of fat in the liver. According to the research, alterations in the methylation of the PPARγ promoter are crucial to the development of NAFLD, thereby accentuating the intricate interplay between dietary habits and epigenetic regulation of metabolic diseases. [95]

In terms of histone modifications, another study in primates has shown that a maternal HFD can cause modifications in histone acetylation patterns in the fetal liver, leading to changed gene expression levels, implying the possibility of a mechanism through which nutrition may affect a child's vulnerability to disease. [96] Transgenerational epigenetic effects can also be observed upon treatment with a HFD. According to several research articles, the consequences of a maternal HFD persisted even in third generation female progeny and could be passed down via the paternal lineage. [97] A similar study highlighted that fathers on an HFD can pass on altered sperm cell histone modifications, regulating the expression of tissue specific genes in the liver of their male offspring, suggesting the transgenerational epigenetic effects of dietary choices. [98]

As mentioned in section 4.3.2, parental obesity in *C. elegans* can lead to histone H3K4 trimethylation (H3K4me3), which is responsible for marking genes related to lipid metabolism, including transcription factors DAF-16/FOXO and SBP-1/SREBP, nuclear receptors NHR-49 and NHR-80, and δ-9 desaturases (*fat-5*, *fat-6*, and *fat-7*). Lipid accumulation in *C. elegans* offspring is regulated through epigenetic inheritance and an upregulation of metabolism genes due to obesity influences. [60]

By the aid of high-throughput techniques in genetic engineering and lipidomics, it has been shown that changes in lipid metabolism are closely connected to aging and its associated diseases. According to studies, the equilibrium between lipid metabolism, body adiposity and its metabolites play a crucial role as regulators of gene expression in signaling networks related to ageing. [99] Moreover, according to recent researches, several membrane lipids are essential for cellular signaling and signal transduction, meaning that any imbalance in their metabolism could result in illness. Since these lipids have an effect on physiological processes, they can serve as biomarkers for disease diagnosis and treatment. Essentially, membrane lipids affect cellular activation and generate a variety of lipid mediators with long-lasting effects. [100]

Lastly, studies have introduced the concept of epigenetic reprogramming and long-lasting effects of dietary habits. A study by Butruille et al. investigates this concept in response to a HFD in mice. White adipose tissue (WAT) formation and the risk of adult obesity are both influenced by the early lactation-suckling stage. In this study, researchers examined the effect of the mother's high-fat dietary habits during lactation on their male offspring's fat tissue development. The findings demonstrated that whereas maternal HF eating didn't induce any changes on the mother's weight or the general composition of her

breast milk, it did however modify the fatty acid content of the milk, leading to increased infant weight, fat tissue growth and an increased risk of obesity in adulthood, particularly in fat tissue depot (eWAT). This suggests that early postnatal diet, especially fatty acids found in breast milk, might regulate long-term fat tissue formation, due to an epigenetic modification in a crucial fat metabolism enzyme, SCD1. [101]

In summary, the connection between a high-fat diet and epigenetic alterations is a focal point of nutritional and genetic research. The epigenome and consequent gene expression are greatly influenced by dietary habits, particularly those high in fats. Understanding the precise molecular pathways will be crucial for creating dietary recommendations and therapies for disorders linked to nutrition as we continue to investigate this connection.

4.4.3. High-fat diet and cellular stress responses

Beyond the observable and direct physiological consequences of dietary habits, it is important to investigate their implications on a cellular level. A high-fat diet, as described above, can act as a stressor factor, inducing a plethora of cellular stress responses, like heat shock response, autophagy, DNA damage response, unfolded protein response, senescence, inflammatory response and oxidative stress response, to name a few. Upon interaction with a specific stressor, one or more of these cellular can be activated, in order to ensure integrity and protection. [102–104] In our study, we are particularly investigating the oxidative stress response in *C. elegans*, triggered by an excessive intake of dietary fats.

Oxidative stress is a physiological imbalance that develops in response to external or internal stressors and disrupts the equilibrium between the number of reactive oxygen species (ROS) and the body's capacity to detoxify or repair the harm they cause. ROS are oxygen-containing molecules that have one or more unpaired electrons and are naturally created by several metabolic cellular processes, particularly in mitochondria. [105]

Generation of ROS primarily occurs in mitochondria, during the process of oxidative phosphorylation. The mitochondrial electron transport chain (ETC) is traversed by electrons in multiple protein complexes. A premature reaction between electrons and molecular oxygen, leads to the formation of superoxide, a main ROS. Other ROS forms, including hydrogen peroxide, can subsequently be produced from superoxide. Although this is a consequence of cellular respiration, uncontrolled ROS levels can be harmful, highlighting the significance of equilibrium maintenance *(Figure 18)*. [106]

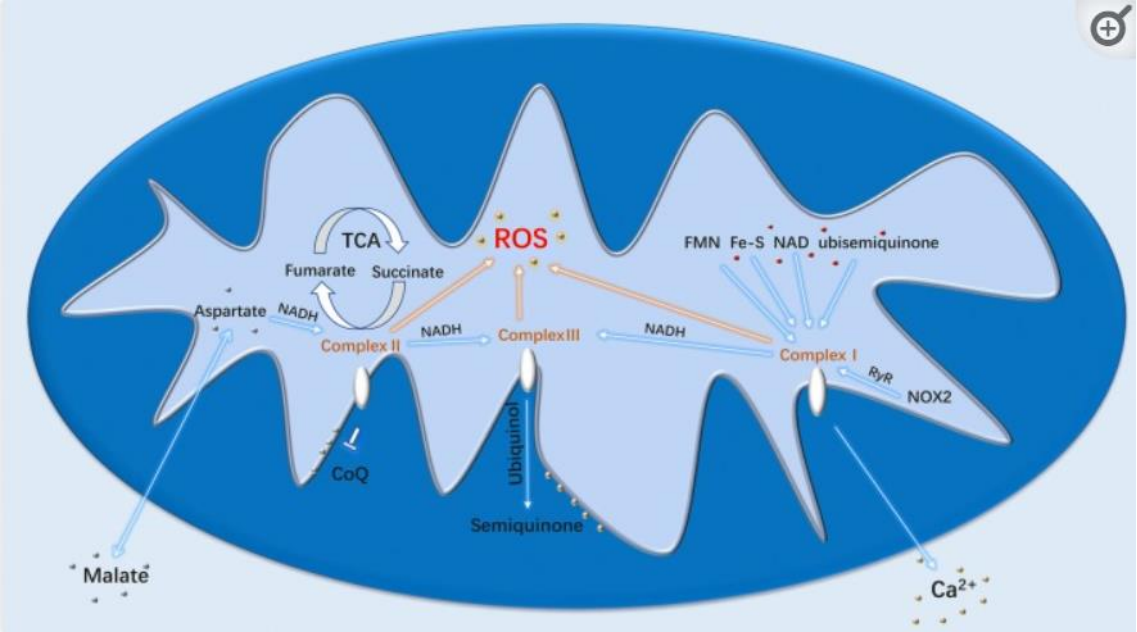

Figure 18 Generation of ROS in mitochondria (Source: Yang et al., 2020*)*

The NOX family of enzymes, often known as NADPH oxidases, also constitutes a key generator of ROS. These enzymes, designed particularly for the formation of ROS, transport electrons from NADPH to oxygen, resulting in the creation of superoxide and other ROS. NOX enzymes are found in a variety of cell types and are involved in a wide range of activities, including immunological and cellular signaling. However, their downregulation can result in illnesses like cardiovascular disorders. [107]

ROS can also be generated endogenously by the immune system, for defense purposes. The "respiratory burst", as it is called, is a mechanism wherein immune cells, particularly neutrophils and macrophages, release increased levels of ROS when they come into contact with pathogens. Invaders are successfully neutralized by this process, but prolonged ROS generation may unintentionally harm host tissues. [108]

Even though ROS are crucial for immune system and cell signaling function, exceedingly elevated amounts of them might be harmful for cells in the long run, resulting in a number of chronic illnesses, such as cancer, cardiovascular diseases, neurological and metabolical disorders. This is due to their high chemical reactivity with other cellular components. ROS can be very detrimental, as they can lead to lipid peroxidation, protein carbonylation, DNA strand breaks, decreased ATP production due to electron transport chain implications and activation of apoptosis pathways *(Figure 19)*.[109]

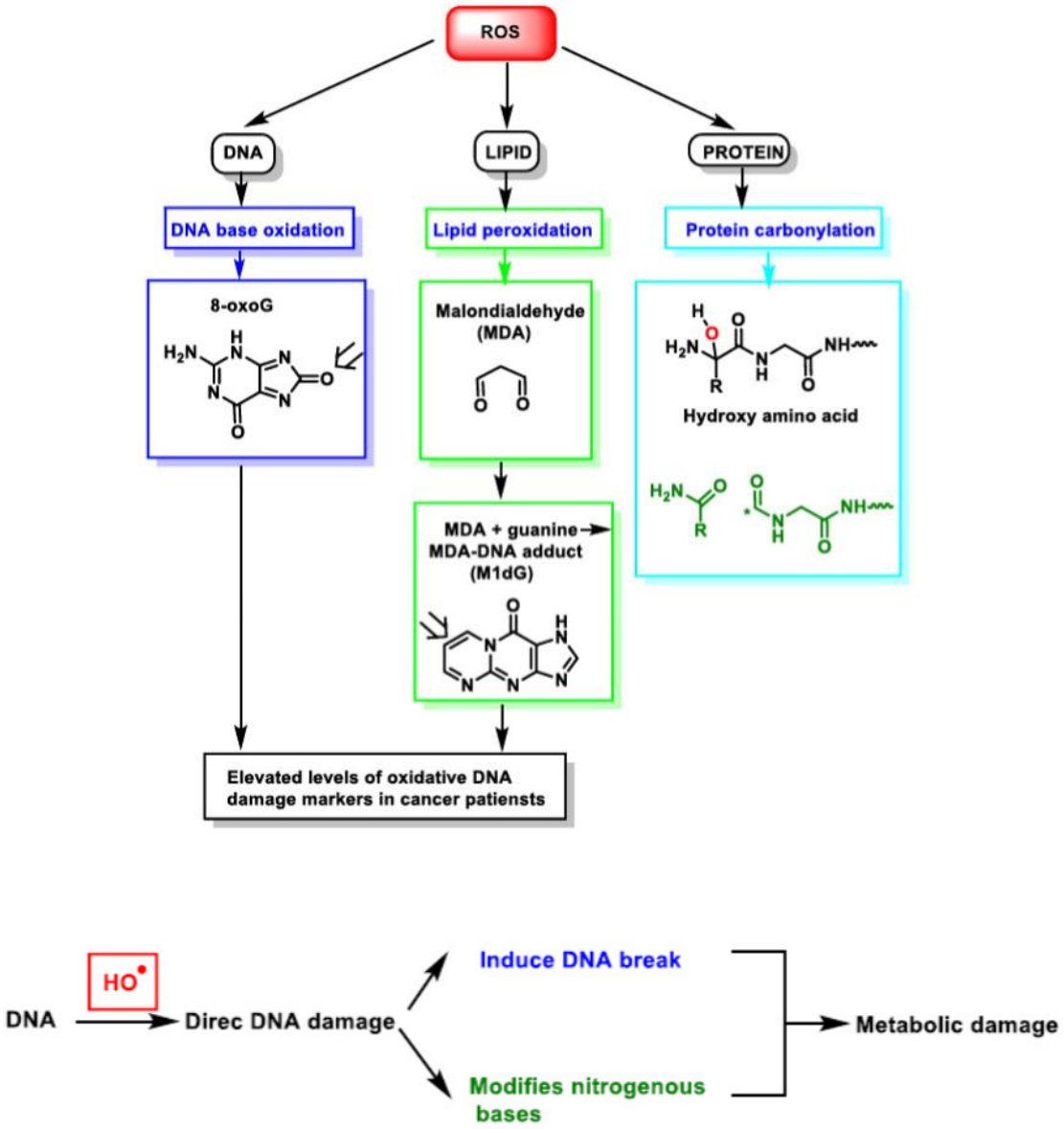

Figure 19 A) ROS action on DNA, lipids and proteins lead to DNA base oxidation, lipid peroxidation and protein carbonylation, respectively. * Unpaired electron. B) DNA damage caused by ROS. (Source: Juan et al., 2021)

Cells have developed multiple defense antioxidant mechanisms that counteract ROS, when their concentration levels surpass the cell's capability of neutralizing them. The most common one is redox (reduction-oxidation) detoxification, which is carried out by special enzymes, responsible for various processes including signaling, detoxification, and energy generation. The purpose of these enzymes is electron transport between molecules, so as to achieve ROS elimination or regulation of particular cellular pathways. [110] Harmful superoxide radicals (O_2^-) are converted into less harmful hydrogen peroxide (H_2O_2) and molecular oxygen (O_2) by the enzyme SOD (superoxide dismutase). Subsequently, other

enzymes, like catalase, can further break down hydrogen peroxide into water and oxygen, ensuring that ROS levels are efficiently controlled within the cell *(Figure 20)*. [111]

According to current bibliography, several studies have demonstrated that a HFD significantly affects the production and accumulation of ROS. A HFD disrupts lipid metabolism, increasing oxidative stress and the products of lipid peroxidation. For downstream signaling pathways to be activated, fatty acids synergistically interact with a number of transcriptional factors. Peroxisome proliferator-activated receptor (PPAR), a ligand-activated transcription factor, is a transcriptional molecule that serves as a sensor for proteins that regulate lipids. [112,113] This increased oxidative stress has been linked to a number of health issues, such as inflammatory illnesses, insulin resistance, and cardiovascular conditions. Increased ROS levels brought on by a HFD can be used as possible therapeutic targets and diagnostic markers for diseases related to obesity. Additionally, the ROS-induced oxidative stress caused by a lipid diet may interfere with other physiological pathways, thereby escalating their negative effects and further disrupting cellular homeostasis. [114]

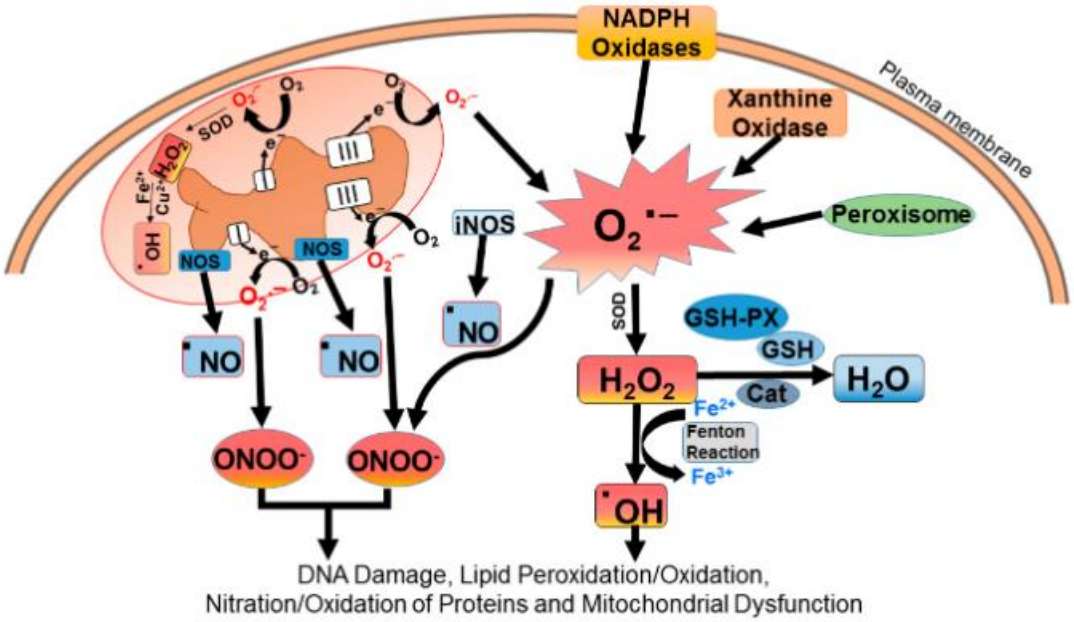

Figure 20 Generation of reactive oxygen species (ROS) in the cell. ROS are generated by enzymatic and non-enzymatic redox reactions during cellular metabolism under normal and pathological conditions. Mitochondria, plasma membrane, peroxisomes, and cytosol first generate the superoxide anion (O2•−), which becomes the precursor free radical for the generation of other ROS molecules. Cytosolic CuZN superoxide dismutase (SOD) and mitochondrial MnSOD, which are expressed in the kidney, dismutate O2•− to H2O2, which yields highly reactive hydroxyl radicals (OH•) by interaction with reduced transition metal ions (such as Fe and Cu) in a Fenton reaction. In addition to ROS, cells also generate reactive nitrogen species (RNS). The major RNS include nitric oxide (•NO), peroxynitrite (ONOO−), and nitrogen dioxide (•NO2). Nitric oxide (•NO) is produced by three isoforms of nitric oxide synthase (NOS), all of which are expressed in the kidney. ROS produced cause oxidative damage, including DNA damage, lipid and protein oxidation, protein nitration, and mitochondrial dysfunction. (Source: Kaushal et al., 2019)

5. Work hypothesis

Modern societies face a wide range of nutritional and metabolic challenges, as a result of rapidly changing lifestyles and eating habits. These lifestyle adjustments have been connected to a variety of health issues, ranging from metabolic disorders to age-related diseases. The intricate molecular mechanisms by which dietary variables affect epigenetic landscapes and, therefore, modulate metabolism have only recently begun to be unraveled in existing scientific literature. Epigenetic regulators like histone deacetylases and methyltransferases, which control how organisms sense and respond to dietary signals, have emerged as fundamental components in lipid metabolism. [115–119] However, there is a conspicuous knowledge gap about how specific epigenetic modifiers or chromatin marks govern the transcription of genes associated with diverse facets of lipid metabolism and interact with dietary cues, in particular a high-fat diet (HFD). Our study aims to bridge this lacuna, by disrupting genes encoding one histone deacetylase and four methyltransferases, in order to gain valuable insights into the function and regulation of metabolic genes in *C. elegans*, upon exposure to a HFD. To achieve this, we used N2 wild-type worms along with various knockout strains targeting genes such as *hda-2, set-4*, *set-14*, *set-18* and *set-30* respectively. Our aim is to shed light on the molecular mechanisms driving diet-induced epigenetic modifications and their general implications in ageing and metabolic health. Here, we observe the resulting phenotypic changes by examining longevity and mitochondrial homeostasis (mitoROS levels), in response to a diet rich in monounsaturated fatty acids.

6. Materials and Methods

6.1. Bacterial strains

Feeding and maintenance of worms was achieved using *Escherichia coli* strain OP50, obtained from the Caenorhabditis Genetics Center (CGC) for the conventional use as a food source in laboratory settings. (Genotype: *E. coli,* uracil auxotroph)

6.2. Medium for bacterial cultures

Luria- Bertani (LB) is a versatile nutrient-rich medium utilized in a plethora of microbiology techniques for the culture and growth of various bacterial strains, including *E. coli* OP50. Despite its use for general bacterial culturing, it can also serve as a medium for maintaining bacterial stocks for later use. LB medium can be prepared in both solid (agar- based) and liquid forms, depending on the desired use.

Liquid LB

To prepare LB medium in liquid form, 20g of sodium chloride (NaCl), 20g of Tryptone, and 10g of yeast extract are dissolved in 1800mL distilled H_2O. We stir the mixture until we achieve complete homogeneity. Then, we adjust the pH to 7.0 by adding sodium hydroxide (NaOH) and we adjust the volume to 2L with H_2O. We dispense the liquid LB into conical flasks of 100mL and 200mL and we sterilize them by autoclaving.

Solid LB

For the preparation of solid LB medium, we mix the ingredients described above with 30g of agar powder in 1500mL distilled H_2O. Agar powder is not easily dissolved until after autoclaving. We, then, adjust the pH to 7.0 using NaOH and we sterilize by autoclaving. After autoclaving, we bring the volume to 2L with sterile H_2O. After the medium cools down to approximately 50˚C, we dispense 17mL of LB into standard petri plates (92mm diameter x 16mm height). Ampicillin can be added at a final concentration of 100μg/mL before dispensing to prepare plates for ampicillin-resistant clones.

6.3. Culturing conditions of *E. coli* OP50 bacteria

In order to culture *E. coli* OP50 bacteria in liquid LB medium we follow a standard procedure. Firstly, we grab a sterile flask containing fresh and autoclaved LB medium. After ensuring an aseptic environment, we obtain a single colony from an OP50 agar plate by using a sterile pipette tip. Then, we inoculate the liquid LB by dispensing the sterile tip inside the flask. To guarantee adequacy of nutrients for growth, the volume of the inoculum should be small compared to that of the medium. Subsequently, we transfer our flask for incubation at 37^{o}C, to achieve optimal growth conditions. The duration of incubation may vary according to factors such as initial number of cells or distinct experimental requirements. For that reason, we monitor bacterial growth periodically, until desired cell density is reached. When ready, OP50 culture can be harvested and used for worm maintenance and handling. If necessary, flasks of OP50 liquid cultures can be stored at 4^{o}C for short-term storage.

6.4. Bacterial stabs

Bacterial stabs serve for long-term storage of bacterial cultures. In our case, we have preserved the *E. coli* OP50 bacterial strain. We did so by harvesting 1mL of liquid OP50 culture and mixing it with 1mL of sterile glycerol 80% v/v inside a cryovial (1:1 ratio). After ensuring secure sealing, we transfer the vial at -80^{o}C and freeze them as glycerol stocks.

6.5. Streaking of bacterial strains

Streaking of bacterial strains is done from frozen glycerol stocks (stabs) on LB agar plates. For this study, we aim to grow OP50 *E. coli* single bacterial colonies, that will be later used for inoculation of liquid LB medium.
Firstly, we retrieve the frozen glycerol stock of choice and after ensuring aseptic conditions, we pick a small amount of OP50 using a sterile pipette tip. We continue by streaking the agar plate in four quadrants, in a technique known as T-streak. The main objective of this technique is to thin the colonies as the streaking moves in a clockwise manner. As a result, we can isolate individual OP50 bacterial colonies. Finally, we close the plate and place it in the incubator overnight at 37^{o}C lid-side down. After incubation, we can store the plate at 4^{o}C for no more than 4 weeks.

6.6. Nematode Strains

For the purpose of our research experiments, a total of six worm strains were utilized. All nematode strains listed below are available in the Caenorhabditis Genetics Center and can

be acquired upon order.

1. N2: wild type Bristol isolate

This strain serves as the standard reference for *C. elegans* research and has been extensively characterized and studied over the years.

2. VC997: *set-4* knockout *C. elegans* strain

This is a superficially wild type knockout strain. It was generated by performing EMS mutagenesis, resulting in an out-of-frame allele deletion of the *set-4* gene on chromosome II. Genotype: *set-4*(*ok1481*) II [120]

3. VC983: *hda-2* knockout *C. elegans* strain

This is a superficially wild type knockout strain. It was generated by performing EMS mutagenesis, resulting in an out-of-frame allele deletion of the *hda-2* gene on chromosome II. Genotype: *hda-2*(*ok1479*) II [121]

4. VC767: *set-18* knockout *C. elegans* strain

This is a superficially wild type knockout strain. It was generated by performing gamma ray-induced mutagenesis, resulting in a loss of function allele of the *set-18* gene on chromosome I. Genotype: *set-18*(*gk334*) I [122]

5. VC719: *set-30* knockout *C. elegans* strain

This is a superficially wild type knockout strain. It was generated by performing gamma ray-induced mutagenesis, resulting in a loss of function allele of the *set-30* gene on chromosome X. Genotype: *set-30*(*gk315*) X [123]

6. RG3241: *set-14* knockout *C. elegans* strain

This is a homozygous viable knockout strain. A deletion with Calarco/Colaiacovo selection cassette was performed in the *set-14* gene on chromosome II using CRISPR/Cas 9 as a mutagen. Several elements were introduced into the *set-14* gene, including LoxP sites for targeted DNA recombination, a GFP coding sequence under the control of the *myo-2* promoter and a *neoR* gene under the control of the *rps-27* promoter. The *neoR* gene confers resistance against the antibiotic neomycin and serves as a selectable marker during selection of transgenic worms. Genotype: *set-14*(ve741[LoxP + *myo-2p::*GFP*::unc-54* 3' UTR + *rps-27p::neoR::unc-54* 3' UTR + *LoxP*]) II [124]

The above mentioned mutant strains have not yet been extensively studied. Due to lack of scientific literature, little is known about their descriptive phenotypical characteristics.

6.7. Buffers for *C. elegans* experiments

M9 minimal medium

The M9 buffer is a commonly used solution in several procedures of *C. elegans* handling and maintenance. It is preferred over distilled sterilized water, because it meets the requirements for a standardized environment, in terms of pH levels and osmolarity.

For the preparation of 1L of M9 medium we dissolve 3g of potassium phosphate dibasic (KH_2PO_4), 6g of disodium phosphate (Na_2HPO_4) and 5g of sodium chloride (NaCl) in 900mL distilled H_2O. We proceed to sterilize our solution. After autoclavation, the solution must be left to cool down until it reaches RT. Subsequently we add 1mL of magnesium sulfate ($MgSO_4$) from a stock solution with a concentration of 1M. Lastly, we adjust the volume to a total of 1L by pouring sterile H_2O.

Bleaching solution

The bleaching solution is used to selectively kill and melt the bodies of adult animals, in order to harvest their eggs or newly hatched larvae.

For the preparation of 10mL of bleaching solution we add 1mL of sodium hydroxide (NaOH) from a 5N stock solution and 2mL of sodium hypochlorite (NaOCl) 5% v/v in 7mL sterile H_2O.

Levamisole solution

Levamisole is used in the context of *C. elegans* imaging as an anesthetic to immobilize the worms, facilitating in vivo studies and imaging.

For the preparation of 100mM of stock solution, we dissolve 24.076 g of levamisole hydrochloride (molecular weight: 240.76 g/mol) in 500mL M9 buffer with stirring. The solution was then transferred to a volumetric flask and the volume was brought to a final of 1L by adding M9. The stock solution was stored in an amber-colored container.

In our imaging experiments, we use 20mM levamisole solution aliquots. To prepare 10mL of the diluted solution, we obtain 2mL of the 100mM stock solution and add 8mL of M9 buffer.

Nematode Growth Medium buffers

- $CaCl_2$ 1M solution: For the preparation of 1M stock solution, we weigh out 14,7g of calcium chloride dihydrate ($CaCl_2 \cdot 2H_2O$) needed for a solution of 100mL (M.W

147,02g/mol). We dissolve the salt in ddH_2O, until our final volume is reached. Finally, we sterilize the solution by autoclaving. The solution should be stored at room temperature in a cool, dry place away from direct light.

- $MgSO_4$ 1M solution: For the preparation of 1M stock solution, we weigh out 24,65g of magnesium sulfate heptahydrate ($MgSO_4 \cdot 7H_2O$) needed for a solution of 100mL (M.W 246,48g/mol). We dissolve the salt in ddH_2O, until our final volume is reached. Finally, we sterilize the solution by autoclaving. The solution should be stored at room temperature in a cool, dry place away from direct light.

- KPO4 1M solution: For the preparation of 1M stock solution, we weigh out 204.4g of potassium phosphate monobasic (KH_2PO_4) and 114.12g of potassium phosphate dibasic (K_2HPO_4) needed for a solution of 2L. We dissolve both compounds in ddH_2O, until our final volume is reached. We mix thoroughly to ensure homogeneity. Finally, we sterilize the solution by autoclaving. The solution should be stored at room temperature in a cool, dry place away from direct light.

- Cholesterol 5mg/mL solution: To prepare a 5mg/mL cholesterol solution with a final volume of 200 mL, we weigh out 1g of cholesterol powder and we dissolve it in 200mL ethanol (100% v/v). We mix the solution thoroughly to ensure homogeneity. The solution must be stored in a cool, dark place, preferably at 4^oC.

- Nystatin 10mg/mL solution: To prepare a 10mg/mL nystatin solution with a final volume of 200 mL, we weigh out 2g of nystatin powder and we dissolve it in 200mL ethanol (70% v/v). We mix the solution thoroughly to ensure homogeneity. The solution must be stored in a cool, dark place, preferably at 4^oC.

6.8. Nematode culture conditions

Standard nematode culture conditions

All *C. elegans* strains used in this study were maintained in standard NGM plates seeded with a bacterial lawn of OP50 *E. coli*.

The protocol we followed for the preparation of 2L of Nematode Growth Medium plates is described below.

1. In a 2L conical flask we dilute 6g of NaCl, 5g of Bacto-peptone, 34g of agar and 0.4g Streptomycin in 1500mL distilled H_2O. (We make sure not to add Streptomycin when intending to perform RNAi assay experiments).
2. We mix thoroughly using a stirrer magnet until it becomes homogenous.
3. We sterilize the mixture by autoclaving and we wait until it cools down to 55^oC.

4. Subsequently we add 2mL of $CaCl_2$ (1M stock solution), 2mL of $MgSO_4$ (1M stock solution), 50mL of KPO_4 (1M stock solution), 2mL cholesterol (5mg/mL stock solution) and 2mL nystatin (10mg/mL stock solution).
5. We adjust the volume to 2L with sterile H_2O and we stir for a few more seconds.
6. Liquid NGM is then dispensed to petri plates. The amount of NGM that is poured varies relative to the size of the petri dishes used. For example, general maintenance of worms is executed on 60mm diameter plates. Plates of 100mm diameter size are mostly preferred when large amounts of worms are needed for a particular experiment. Consequently, approximately 7mL and 17mL of liquid NGM are poured in each plate, respectively.
7. Petri plates are left to dry off at RT for at least 24 hours.

After solidification, NGM plates are ready to be seeded with liquid OP50 *E. coli* bacterial culture. For the 60mm diameter plates, we add approximately 250μL per plate, whereas for the 100mm diameter plates, we pipette 500μL of liquid OP50 culture per plate. Seeded plates are incubated overnight at RT. When worms reach the desired developmental stage (usually L4 larval stage), they can be directly transferred on the surface of the OP50-seeded NGM plates using a platinum pick. After approximately 3,5-4 days, next generation L4 stage worms will have occurred and must be transferred to new seeded NGM plates, in order to avoid starvation and, therefore, accumulation of epigenetic modifications. Time needed for a full life cycle of *C. elegans* (from L4 to L4) varies from strain to strain.

Worm-containing NGM plates are typically maintained at a constant temperature of 20^{o}C. To avoid overcrowding and preserve the genetic purity of worm populations, *C. elegans* cultures require routine care, which includes sub-culturing and occasional transfers to fresh NGM seeded plates.

High Fat Diet (HFD) nematode culture conditions [experimental approach]

For the purpose of our experiments all worm strains are treated within two distinct conditions: standard diet (control animals) and high-fat diet (treated animals).

Under standard dietary conditions, worm strains are cultured as described above, with the only variation being in the OP50-seeded NGM plates. Prior to worm transfer, all seeded NGM plates are placed inside a UV chamber for approximately 15 minutes. UV radiation is responsible for killing the live bacterial lawn, that worm strains will later feed on.

Under high-fat dietary conditions, worm strains consume a special mixture composed of egg yolk particles and UV killed OP50 liquid culture.
To make the high-fat diet mixture, we firstly boil an egg for 12 minutes until it hardens. After ensuring an aseptic environment, we collect the hardened egg yolk and smash it into a paste.

In a sterile falcon, we add the egg yolk paste until it reaches a volume of 5mL. Subsequently, we pour a UV killed OP50 liquid culture and we bring the final mixture volume to 30mL. We mix by using a vortex device, in order to establish consistency and uniformity.

The mixture was prepared at a ratio of 1 part egg yolk and 5 parts liquid OP50 bacterial culture. Killing of OP50 bacteria using UV radiation was done to prevent the live bacteria from interfering with or digesting the egg yolk components. The egg yolk contains lipids and nutrients that are intended to be a supplemental food source for the *C. elegans* worms. Thus, if the OP50 bacteria were alive, they could potentially consume or metabolize the nutrients present in the egg yolk. Therefore, in this way we exclude the possibility of measuring the effect of their metabolic byproducts in the worms' metabolism. The mixture can be stored at 4^{o}C for no more than two weeks.

When seeding NGM plates using this mixture, plates must be left to dry for a few minutes. These plates may later be used to sustain and propagate *C. elegans* populations under high-fat dietary conditions throughout the experimental duration.

Both in the control and treated animal groups, cultivation for all nematode strains starts at the developmental stage of the egg.

6.9. Bleaching and synchronization of *C. elegans* population

Bleaching is a commonly used method when performing *C. elegans* experiments. Its main purpose is to synchronize worm populations. This allows for collection of a synchronized population of *C. elegans* eggs, which can be hatched into a uniform cohort of worms at the same developmental stage. Secondarily, the bleaching technique aims to eliminate undesired contamination, which can result in misleading experimental outcomes. The process involves using a sodium hypochlorite solution to selectively kill the adult worms and their progeny, while leaving the incorporated eggs intact. The protocol we follow is described below.

1. Use 1mL-2mL (depending on the number of plates to be bleached) of M9 solution and wash NGM plates containing gravid hermaphrodite worms. Nematodes must not be older than Day 3 adults.
2. Collect the worm-containing liquid in an Eppendorf tube.
3. Centrifuge for 15s at 3000rpm and discard the supernatant.
4. Repeat the wash by using sterile ddH_2O
5. Add approximately 700μL of bleaching solution directly to the worm pellet.
6. Shake well by hand or vortex for strictly 5-6 minutes, or until there are no visible worm bodies. By then, only eggs should be visible, while the worm bodies should have been completely dissolved.
7. Centrifuge for 30s at 3000rpm and carefully discard the supernatant without disturbing the egg pellet.

8. Wash the pellet twice with 500μL sterile ddH_2O or M9.
9. Dissolve the eggs in an appropriate volume of sterile ddH2O or M9, according to egg density.
10. Transfer the desired amount of eggs in either OP50-seeded plates or NGM plates containing the high-fat diet mixture and store at 20^oC until hatching.

A setback of this procedure is that the resulting worm population is not completely synchronized, because there might be unhatched eggs with a 5 or 6-hour difference.

To overcome this problem, approximately 10 adult hermaphrodites (Day 1 or Day 2) could be transferred to seeded NGM plates in order to lay eggs for a small time frame, circa 1 hour. In such wise, we could achieve better worm synchronization for our experiments.

6.10. RNA extraction from *C. elegans*

In this study, we extracted total RNA from L4 stage worms of our experimental treatments. For total RNA extraction we followed the protocol described below.

1. Pick up L4 stage worms in an Eppendorf tube containing M9 buffer by using a hair-supplemented toothpick.
2. Centrifuge for 1 minute at 14.000rpm
3. Remove the supernatant and wash once again with M9.
4. Remove M9 and add 250μL of Trizol™ reagent.
5. Mix by hand for 30 seconds and then vortex for 4 minutes
6. Store samples at -80^oC
7. The next day, incubate samples at 65^oC for 5 minutes
8. Add 50μL chloroform ($CHCl_3$) [1V to 5V Trizol™]
9. Vortex for 15 seconds and incubate at RT for 3 minutes
10. Centrifugation at 12.000rpm for 15 minutes at 4^oC
11. Transfer the clear layer to a new sterile Eppendorf tube and repeat the above steps after adding chloroform ($CHCl_3$) again [1V to 5V Trizol™]
12. Add 125μL isopropanol and mix by inverting *(can be stored at -80^oC)*
13. Incubate at RT for 3 minutes
14. Centrifugation at 12.000rpm for 10 minutes at RT
15. Discard the supernatant and add 500μL of ethanol 70% v/v [2V]
16. Centrifugation at 14.000rpm for 5 minutes at 4^oC
17. Remove the supernatant and air dry pellet in hood
18. Resuspend the pellet in 20μL RNAse-free H_2O
19. Quantification of RNA concentration using a spectrophotometer. A desired RNA concentration would be between 100ng/μL and 1000ng/μL
    The purity of the extracted RNA can be evaluated by determining the ratio of absorbance readings at 260nm and 280nm (A260/A280). Pure RNAs have a ratio 1.9~2.1.

20. Long term storage of samples at -80°C and short term storage at -20°C

6.11. cDNA synthesis and Real Time- Quantitative Polymerase Chain Reaction

Following total RNA extraction from nematodes, we perform cDNA synthesis using the iScript™ cDNA Synthesis Kit (Bio-Rad). In this experiment, separate PCR micro tubes were utilized for each sample. Our final sample volume was 20μL and the amount of RNA template for each reaction was calculated accordingly, in order to achieve a final cDNA concentration of 1000ng/μL per tube. Reactions took place using a thermocycler, equipped with a suitable protocol for this specific procedure.

RNA template	x μL
iScript™ 5X Reaction Mix	4 μL
iScript™ Reverse Transcriptase	1 μL
RNase-free water	To final volume

The reaction protocol for cDNA synthesis by a thermocycler device is described below:

- 25°C for 5 minutes
- 46°C for 30 minutes (one-step cycle)
- 95°C for 1 minute
- 4°C infinitely

Samples containing cDNA can be stored at -20°C short-termed.

Quantitative Real Time PCR was performed in a Bio-Rad CFX96 Real-Time PCR system, and was repeated three times.
The objective of our Q-PCR reactions was to amplify targeted gene sequences, while simultaneously detecting alterations of gene expression among our samples. Gene expression levels are analogous to the amount of signal emitted by fluorescent dyes and probes, which specifically bind to the amplified DNA.
In this current study, we designed primer pairs for several genes of interest using the BLAST software (Basic Local Alignment Search Tool) provided online by NCBI.

Primer sequences listed below:

Gene	Primer	Primer sequence	Tm °C
skn-1	FW	5'-TCCACCAGGATCTCCATTCG-3'	~59
	RV	5'-CTCCATAGCACATCAATCAAGTCG-3'	~60
hsf-1	FW	5'-CAATCGGCAAGAACTGTGGAGG-3'	~62
	RV	5'-CAAAAGTCTATTTCCAGCACACCTCGT-3'	~64
sod-3	FW	5'-ATTGCTCTCCAACCAGCGC-3'	~61
	RV	5'-GGAACCGAAGTCGCGCTTAA-3'	~61
daf-2	FW	5'-AGCTCTCGGAACAACCACTG-3'	~59
	RV	5'-TGACAAGTCGAAGCCGTCTC-3'	~59
daf-16	FW	5'-GCGAATCGGTTCCAGCAATTCCAA-3'	~63
	RV	5'-ATCCACGGACACTGTTCAACTCGT-3'	~63
set-30	FW	5'-TTGGAGCTCGCCAATGACAA-3'	~57
	RV	5'-AGACGACAAAGCGTGATCCA-3'	~57
hda-2	FW	5'-TCGTGGAGCACCATCAGTTC-3'	~59
	RV	5'-CCCCAGTACTGACCAATCCG-3'	~61
set-14	FW	5'- ACGGGAAATCCAATCGGTGT-3'	~57
	RV	5'- CTTCCATTCGTGCGTTTCGG-3'	~59
set-18	FW	5'- ACATCTCGCGAACTCTCCG-3'	~59
	RV	5'- AGAACTTGAGTGGCGAACGG-3'	~59
set-4	FW	5'- CGCTGTTCGACTCTATGGCT-3'	~59
	RV	5'- CTGCCGTAGAAGCAGGTGAT-3'	~59
act-1 (housekeeping-reference gene)	FW	5'- AGGCCCAATCCAAGAGAGGTATC-3'	~62
	RV	5'- TGGCTGGGGTGTTGAAGGTC-3'	~62
pmp-3 (housekeeping-reference gene)	FW	5'- CTTGCTGGAGTCACTCATCGTGTTATG-3'	~64
	RV	5'- GTCGGGACGCTGATTTATCATCTTC-3'	~62

6.12. Survival and Lifespan assays in *C. elegans*

Lifespan assays were performed at the maintenance temperature of 20˚C. Synchronization of worm populations was achieved by bleaching (hypochlorite treatment) a large amount of gravid adults of all knockout strains grown on OP50-seeded NGM plates. Eggs were placed immediately on freshly made HFD and UV-killed OP50 plates. The progeny was grown

through the L4 larval stage and then transferred to fresh plates in groups of 20-25 worms per plate for a total of 150–200 individuals per condition. The day after transferring L4 was used as t=1 (days of adulthood). Animals were transferred to freshly made HFD and UV-killed OP50 plates every 2 days until the 12th day of adulthood and every 3 days until the end of the experiment. This was done in order to avoid confusion of 2nd generation worms with our initial population. The animals were examined almost every day and scored as alive or dead (if they do not respond to touch). Hermaphrodites with internally hatched eggs (bagging), protruding or ruptured vulvas, or those which accidentally die during handling or due to dehydration in the edges of the plate, were scored as censored. Contaminated plates were excluded from scoring. Out of all repetitions, one representative experiment is shown in the corresponding figures. Statistical analysis was performed using the Log-rank (Mantel-Cox) test of the Graph Pad Prism 9 software package.

6.13. Assessment of mitochondrial homeostasis by quantification of mitochondrial ROS (MitoTracker® staining) using fluorescence microscopy

For the determination of mitochondrial Reactive Oxygen Species, L4-staged wild-type (N2) animals, treated with the respective condition since hatching, were transferred on HFD and UV-killed OP50 plates supplemented with 0,10μM MitoTracker™ Red CM-H2Xros. After overnight incubation at 20°, 25-30 animals were transferred to fresh HFD plates and were maintained for 1h, so as to excrete any excess dye that would interfere with our desired signal. After 1 hour, fluorescence imaging of live D1-staged worms was performed. For this specific dye, we aimed to measure a total fluorescence signal emitted from each animal's entire body.
Worms were paralyzed with the use of a 20μl drop of 20mM levamisole on standard microscope slides.
Imaging experiments presented here were performed under the epifluorescent
microscope EVOS FL Auto 2 (Thermofisher Scientific) with a 4x lens. Imaging conditions (e.g. exposure, contrast)
remained consistent throughout each experiment to ensure equal comparability.

6.14. Quantification and Statistical Analysis

Quantification of the mean pixel intensity was performed by using the ImageJ software.

Statistical analysis of all images was performed using the Fiji/ImageJ [125] software platform192. Data were analyzed, visualized, and interpreted using GraphPad Prism 9 software (GraphPad Software, Inc.). Each data set underwent individual testing for normal distribution using the Shapiro-Wilk test. For normally distributed data, one-way ANOVA with

Brown-Forsythe and Welch tests and Dunnet's post-hoc correction were utilized. Data are presented as mean values ± standard deviation (SD) unless mentioned otherwise. For statistical evaluations, *p values* were derived using the unpaired Student's t-test and one-way ANOVA complemented by Tukey's multiple comparison test. Significance levels were set as follows: *($p < 0.05$), **($p < 0.01$), ***($p < 0.001$), and n.s. indicates no significance ($p > 0.1$). For data that weren't normally distributed, the Kruskal-Wallis test and Dunn's post-hoc correction were employed. For two-way ANOVA, Tukey's post-hoc correction was used. Lifespan assays were processed and visualized using Kaplan–Meier analysis.

7. Results

7.1. Treatment with specific high-fat diet affects lifespan of wild-type N2 and knockout *C. elegans* strains

To elucidate the potential effects of dietary interventions on *C. elegans* lifespan, both the wild-type N2 strain and five knockout (KO) strains targeting one histone deacetylase and four methyltransferases were subjected to specific HFD. Upon exposure to HFD, the wild-type N2 strain exhibited a pronounced reduction in lifespan when compared to its lifespan under normal dietary conditions *(Figure 21A)*. Interestingly, a contrasting trend was observed in the KO strains. All five KO strains, irrespective of the targeted gene, displayed a modest increase in lifespan when subjected to HFD, as compared to their lifespan under standard dietary conditions *(Figure 21B - Figure 21F)*. Our mutant strains are outcrossed with our wild-type strain, so as to exclude the possibility of background mutations that could interfere with the observed longevity phenotype. Mean lifespan and statistical significance of each comparison are shown below *(Figure 23)*.

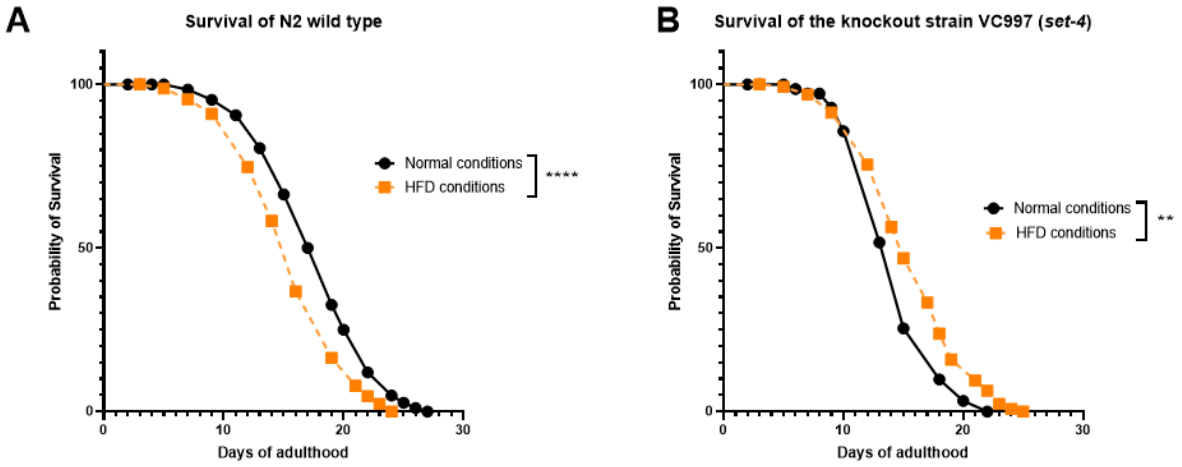

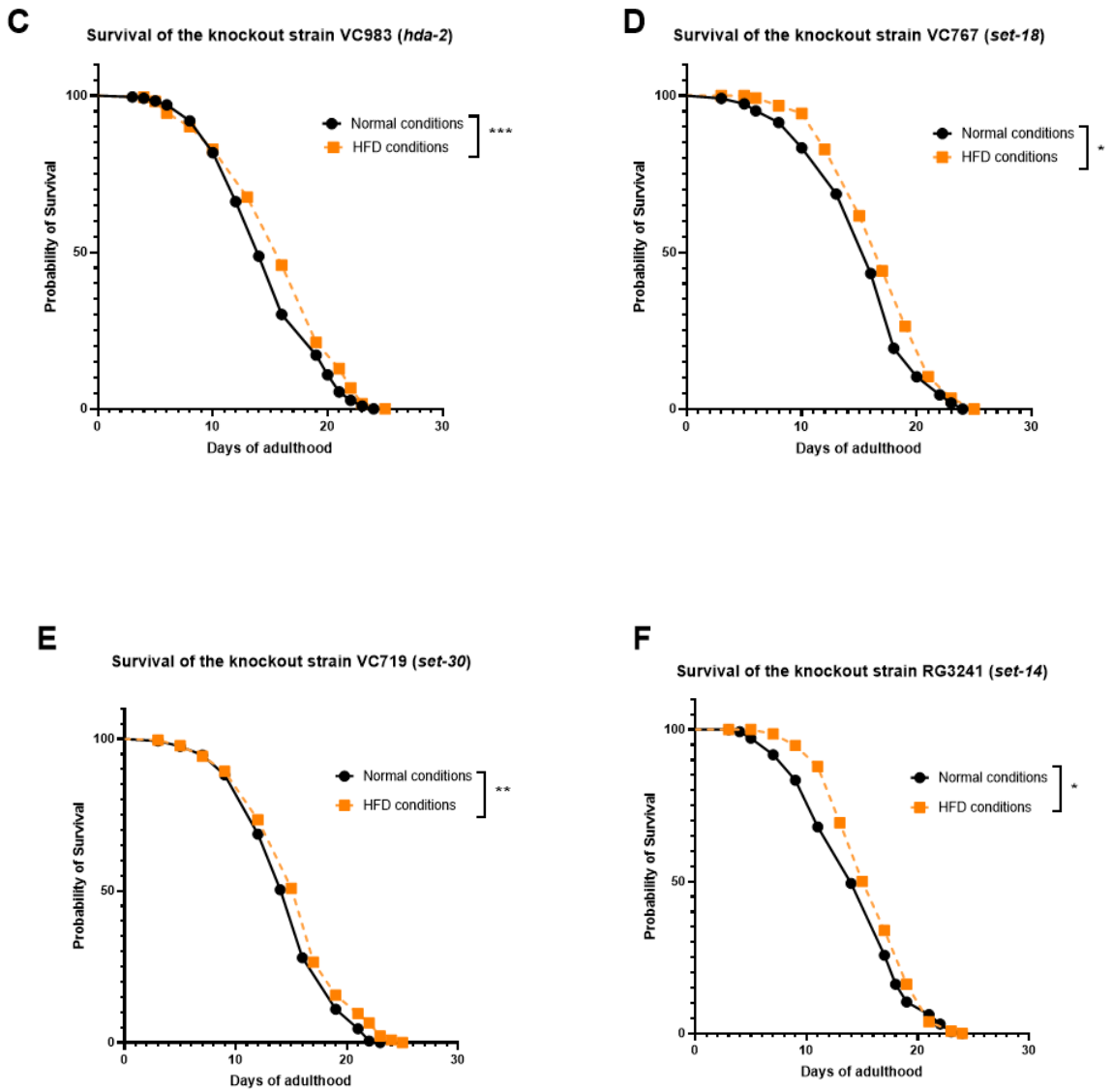

Figure 21 **A-F** Lifespan paired analyses of N2 wild type worms and *set-4*, *hda-2*, *set-18*, *set-30* and *set-14* knockout *C. elegans* strains between normal and high-fat dietary conditions. Survival curves were compared with the Log-rank (Mantel–Cox) test (**** denotes P < 0.0001, *** denotes P < 0.001, ** denotes P < 0.01, * denotes P < 0.05); detailed values are shown in **Figure 24**. Graphs are representative. (N=2)

Under normal dietary conditions, we sought to understand the baseline longevity of different *C. elegans* strains. The wild-type N2 strain served as a reference, exhibiting a mean lifespan of 19 days. In contrast, all knockout strains displayed a significantly reduced mean lifespan *(Figure 22A- Figure 22E)*. Specifically, the VC997 (*set-4*) and VC719 (*set-30*) knockout strains both had a mean lifespan of 15.5 days. The VC983 (*hda-2*), VC767 (*set-18*), and RG3241 (*set-14*) knockout strains all showed a mean lifespan of 15 days *(Figure 24)*.

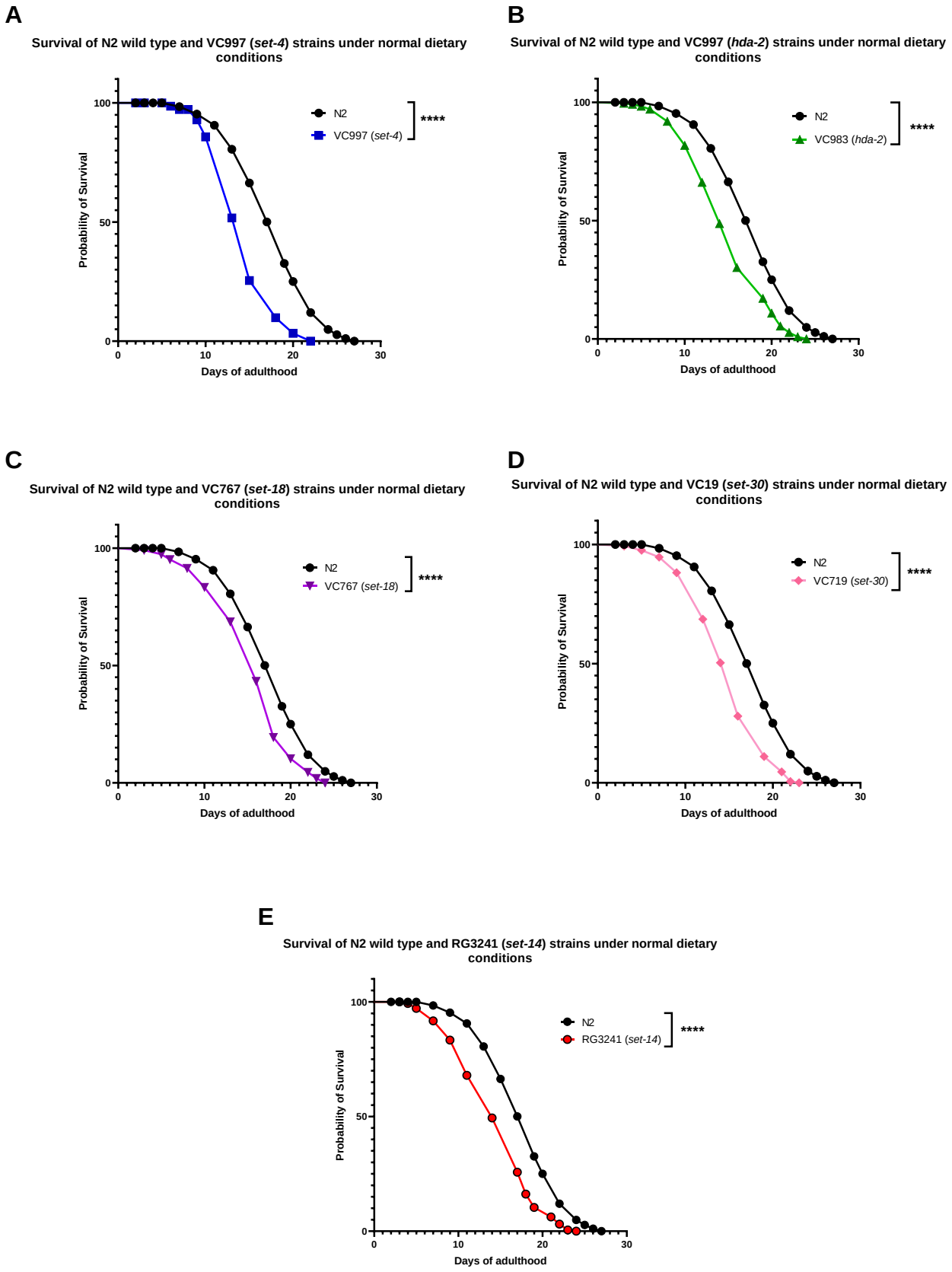

Figure 22 **A-E** Lifespan analyses of all knockout strains under normal dietary conditions compared to N2 wild type. Survival curves were compared with the Log-rank (Mantel–Cox) test (**** denotes P < 0.0001); detailed values are shown in **Figure 24**. Graphs are representative. (N=2)

Longevity of various *C. elegans* strains was also assessed when exposed to HFD. The N2 wild-type strain, which had a mean lifespan of 16 days, served as the reference. Remarkably, most knockout strains displayed lifespans closely aligned with the N2 strain. The VC997 (*set-4*) and VC719 (*set-30*) strains exhibited mean lifespans of 16 and 16.5 days, respectively. Similarly, the RG3241 (*set-14*) strain showed a lifespan of 17 days, while the VC983 (*hda-2*) strain had a slightly reduced lifespan of 15.5 days *(Figure 23A, Figure 23B, Figure 23D, Figure 23 E)*. However, the VC767 (*set-18*) strain showed a significant deviation from the N2 reference *(Figure 23C)* with a mean lifespan of 17.5 days.

Detailed statistical values and significance levels supporting these findings are shown below (Table 1).

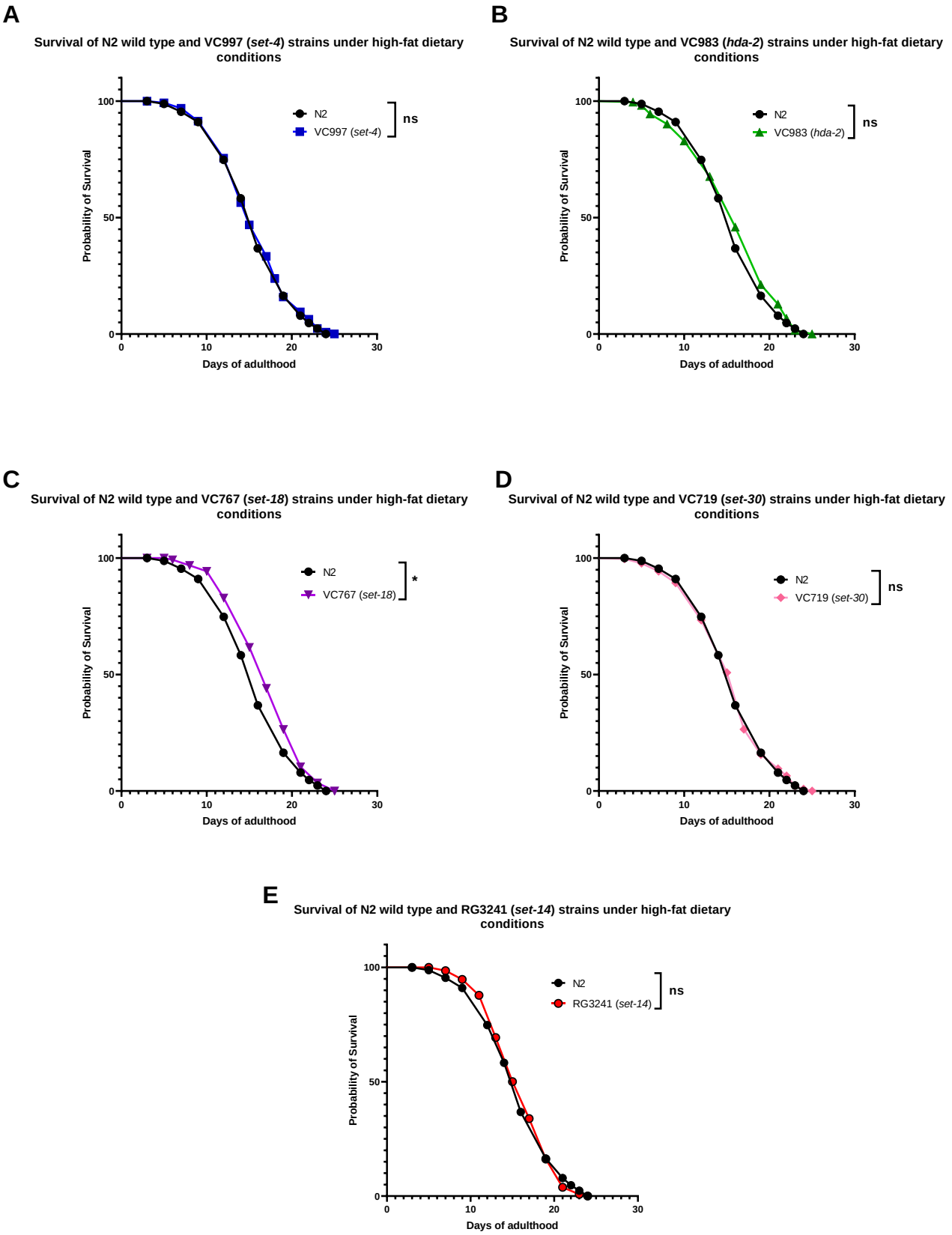

Figure 23 **A-E** Lifespan analyses of all knockout strains under high-fat dietary conditions compared to N2 wild type. Survival curves were compared with the Log-rank (Mantel–Cox) test (* denotes $P < 0.05$); detailed values are shown in **Figure 24**. Graphs are representative. (N=2)

Strain name	Gene knockout	Dietary treatment	Mean lifespan since adulthood (Days)	Number of deaths/ event (n)	P value significance	Ref. control
N2	-	normal diet	19	185		
VC997	*set-4*	normal diet	15.5	127	****	N2 (normal diet)
VC983	*hda-2*	normal diet	15	204	****	N2 (normal diet)
VC767	*set-18*	normal diet	15	180	****	N2 (normal diet)
VC719	*set-30*	normal diet	15.5	208	****	N2 (normal diet)
RG3241	*set-14*	normal diet	15	245	****	N2 (normal diet)
N2	-	HFD	16	187		
VC997	*set-4*	HFD	16	126	**ns**	N2 (HFD)
VC983	*hda-2*	HFD	15.5	199	**ns**	N2 (HFD)
VC767	*set-18*	HFD	17.5	105	*	N2 (HFD)
VC719	*set-30*	HFD	16.5	241	**ns**	N2 (HFD)
RG3241	*set-14*	HFD	17	130	**ns**	N2 (HFD)
N2	-	HFD	16	187	****	N2 (normal diet)
VC997	*set-4*	HFD	16	126	**	VC997 (normal diet)
VC983	*hda-2*	HFD	15.5	199	***	VC983 (normal diet)
VC767	*set-18*	HFD	17.5	105	*	VC767 (normal diet)
VC719	*set-30*	HFD	16.5	241	**	VC719 (normal diet)
RG3241	*set-14*	HFD	17	130	*	RG3241 (normal diet)

Table 1 Summary of lifespan experiments. (N=2)

7.2. High-fat dietary conditions affect the generation of mitochondria-derived reactive oxygen species in wild-type and knockout *C. elegans* strains

Afterwards, we aimed to investigate the role of epigenetic modifiers on oxidative stress. For this purpose, we measured mean fluorescence intensity of 1-day-old animals of all *C. elegans* strains, after overnight supplementation with the selective mitochondrial dye MitoTracker™ Red CM-H2Xros. The wild-type N2 strain, known to have inherently low ROS levels, was used as a negative control. [126] Under normal dietary conditions, all mutant strains exhibited a pronounced increase in ROS levels when compared to the N2 strain *(Figure 25)*. These differences were statistically very significant, as denoted by a significant *p-value* (p< 0.0001).

Interestingly, upon transitioning to HFD, all knockout strains demonstrated a marked reduction in mitochondrial ROS, a change that was again very significant as indicated by the *p-value*. In contrast, the ROS levels in the N2 strain remained more or less constant under HFD. *(Figure 25)*.

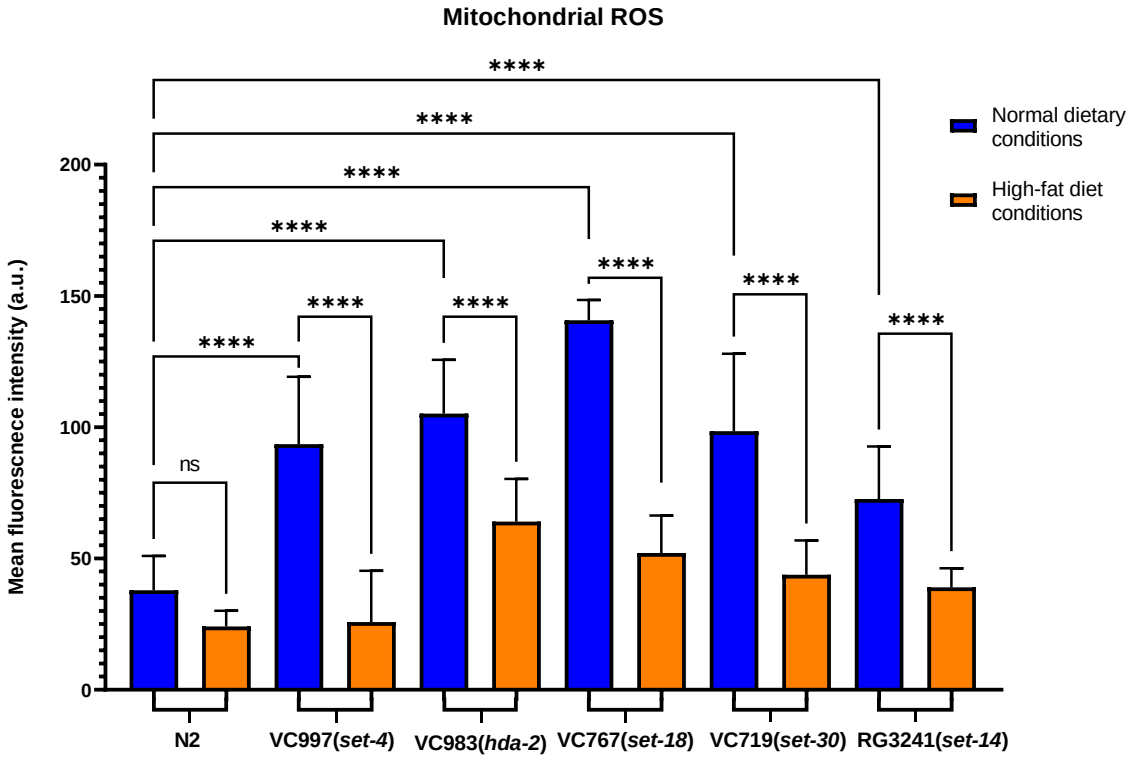

Figure 25 Quantification of mitochondrial ROS (mean fluorescence intensity) in D1 N2 wild-type and *set-4*, *hda-2*, *set-18*, *set-30* and *set-14* knockout *C. elegans* strains treated under normal and high-fat dietary conditions and supplemented overnight with the selective mitochondrial dye MitoTracker™ Red CM-H2Xros. (n=50 animals; **** P<0.0001, One-Way ANOVA). (N=2)

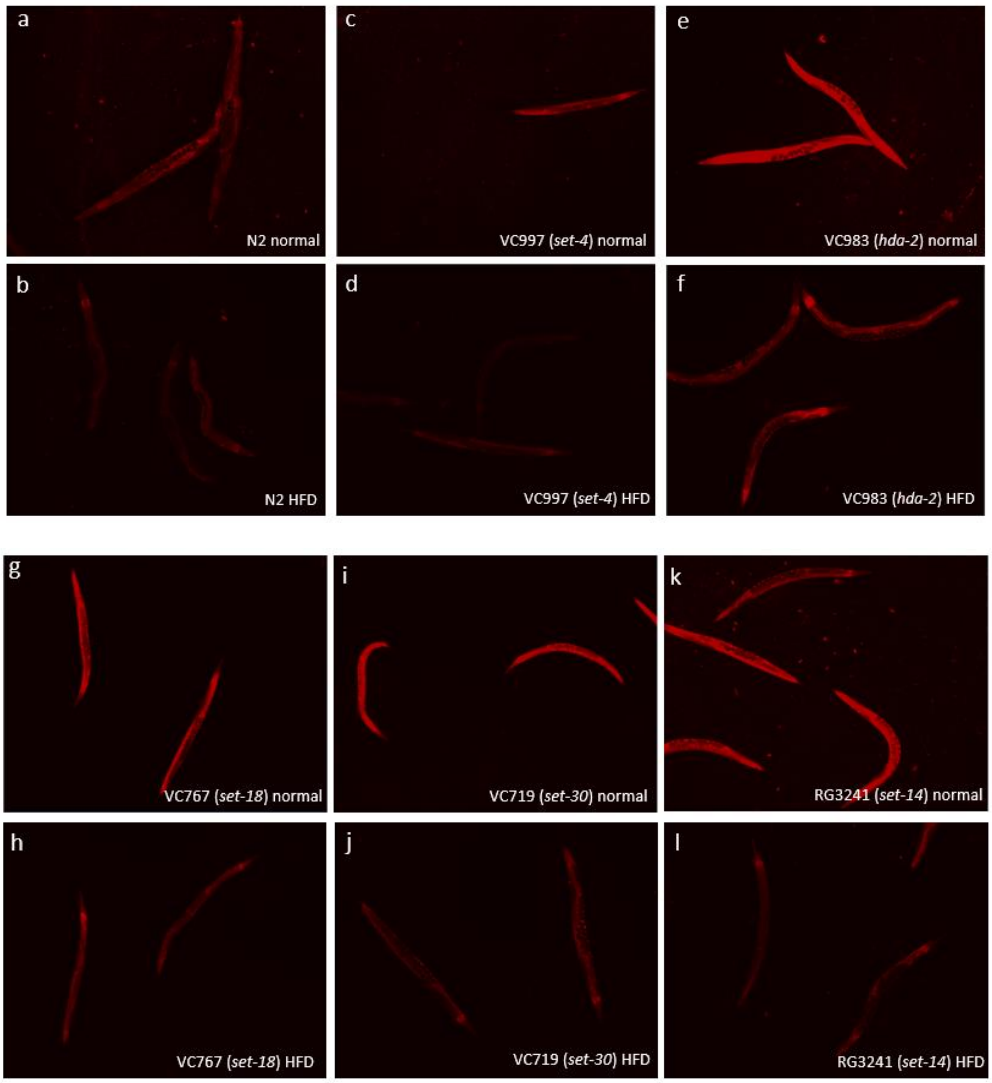

Figure 26 Alterations in mitochondria-derived ROS levels in Day 1 worms of N2 wild-type and *set-4*, *hda-2*, *set-18*, *set-30* and *set-14* knockout *C. elegans* strains treated under normal and high-fat dietary conditions. Fluorescent images are representative.

8. Discussion

In Western nations, metabolic diseases, like obesity, has evolved into an urgent health concern, as confirmed by their epidemic levels of prevalence. The intake of high-calorie, nutrient-poor diets combined with sedentary lifestyles are primarily liable for a nationwide increase in obesity rates. Beyond solely physical health, obesity causes an array of metabolic, cardiovascular, and even neurological disorders as adverse effects. Understanding the molecular and genetic basis of metabolism is of utmost importance, given the enormous impact of dietary habits on health and life expectancy. This has prompted the scientific community to investigate the complex interplay between epigenetic variables and dietary habits. In the context of *C. elegans*, a model organism with genetic and metabolic pathways similar to those of humans, we sought to explore how specific epigenetic factors, represented by our selected mutant strains, influence the organism's metabolic response to HFD and its effects on overall lifespan and healthspan.

Our study provides solid evidence on the differential effects of a specific HFD on the average lifespan of *C. elegans*, with a focus on the wild-type N2 and several knockout strains, targeting a histone deacetylase (*hda-2*) and four methyltransferases (*set-4*, *set-14*, *set-18*, *set-30*).

Under normal dietary conditions, the N2 wild-type strain had a mean lifespan of 19 days (counting since adulthood), which we used as a reference point for our comparisons. Interestingly, under similar conditions, all knockout strains displayed a significantly reduced mean lifespan compared to the N2 wild-type. These findings are in accordance with the well-established roles of histone methyltransferases and deacetylases in regulating longevity, [127–133] suggesting that the lack of these enzymes could render the worms more susceptible to a reduced lifespan.

Upon exposure to HFD, an opposing pattern was revealed. While the N2 wild-type strain showed a significant decrease in lifespan, all mutant strains exhibited a moderate amelioration. This observation suggests that the knockout strains might be inherently resilient to the detrimental effects of HFD, [134,135] potentially as a result of the absence of the histone-modifying enzymes. Notably, only the *set-18* VC767 knockout strain showed a substantial increase in mean lifespan when subjected to a HFD, compared to the N2 wild-type, indicating that SET-18 methyltransferase may play a specific role in moderating the effects of a lipid-rich diet.

Moreover, the evaluation of mitochondria-derived ROS levels in *C. elegans* strains of all treatments was a crucial parameter of our study. Based on currently available scientific research, the N2 wild-type strain can be used as a negative control because it is known to display low levels of ROS in its baseline. [126] Our results further corroborated this, since we observed significant increases in mitochondrial ROS in all mutant strains, in contrast to the N2 wild-type under normal dietary conditions. Nevertheless, upon HFD treatment, all knockout strains, except for the N2 wild-type, displayed an enormous reduction in their ROS levels. The significant reduction in ROS levels after HFD treatment in the knockout

strains may suggest a protective mechanism, accounting for the slight increase in their lifespan observed under HFD conditions.

These observations may be underpinned by a variety of mechanisms. One possible interpretation is that the absence of functional epigenetic regulatory enzymes in the knockout strains, could activate downstream compensatory pathways that offer increased resistance to oxidative stress, especially upon receiving a lipid-rich diet. This could be mediated by enhanced antioxidant defenses or alterations in mitochondrial dynamics and function. The significance of epigenetic alterations is yet another important parameter to take into consideration. Given that the enzymes in question are involved in histone modifications, it is plausible that the chromatin landscapes of the knockout strains have changed, resulting in distinct gene expression profiles that confer resistance to a HFD.

In light of our findings, our work contributes, albeit partially, to the understanding of the complex interplay between epigenetics, lipid metabolism, and ageing in *C. elegans*. While our findings offer insightful observations, a more holistic approach would require comprehensive metabolic assessment. Future perspectives of a more profound understanding could be achieved by evaluating mitochondrial bioenergetics, including measurements of membrane potential, oxygen consumption rates, mitochondrial mass, and lipid accumulation through various staining techniques. Such assessments are crucial because they reveal mitochondrial functional status, which is closely linked to cellular health, energy balance and, therefore, senescence. Furthermore, although we assessed the expression of several important genes by qPCR, including *sod-3* (encoding a key antioxidant enzyme), *hsf-1* (encoding a heat shock transcription factor), *skn-1* (encoding a transcription factor involved in detoxification and stress response), *daf-2* (an insulin/IGF-1 receptor homolog), and *daf-16* (a FOXO transcription factor), we decided not to rely on these results, due to their lack of consistency. In *C. elegans*, these genes are essential in numerous pathways, including stress response, longevity, and metabolic regulation. Their accurate and robust quantification is crucial for a comprehensive view of the ageing process and its modulation by epigenetic and metabolic factors. Owing to the technical challenges encountered, we plan to re-evaluate the expression of these genes in our upcoming studies.

In conclusion, our study highlights the need for further research while shedding light on certain facets of the complex relationship between epigenetics, lipid metabolism, and ageing in *C. elegans*. To confirm and elaborate upon our findings, more repetitions and a wider range of metabolic experiments are imperative.

References

1. Ankeny RA. The natural history of Caenorhabditis elegans research. *Nat Rev Genet*. 2001;2(6):474-479. doi:10.1038/35076538

2. Brenner S. THE GENETICS OF *CAENORHABDITIS ELEGANS*. *Genetics*. 1974;77(1):71-94. doi:10.1093/genetics/77.1.71

3. Markaki M, Tavernarakis N. Caenorhabditis elegans as a model system for human diseases. *Curr Opin Biotechnol*. 2020;63:118-125. doi:10.1016/j.copbio.2019.12.011

4. Palikaras K, Tavernarakis N. Caenorhabditis elegans (Nematode). In: *Brenner's Encyclopedia of Genetics*. Elsevier; 2013:404-408. doi:10.1016/B978-0-12-374984-0.00186-8

5. Byerly. 3. Preparation of growth media 3.1. Preparation of bacterial food source. In: *WormBook*. ; 1976. http://www.wormbook.org/chapters/www_strainmaintain/strainmaintain.html#d0e161

6. Corsi AK, Wightman B, Chalfie M. A Transparent Window into Biology: A Primer on *Caenorhabditis elegans*. *Genetics*. 2015;200(2):387-407. doi:10.1534/genetics.115.176099

7. Johnstone IL. The cuticle of the nematodeCaenorhabditis elegans: A complex collagen structure. *BioEssays*. 1994;16(3):171-178. doi:10.1002/bies.950160307

8. 5.2. Muscles—controlling animal movement. In: *WormBook*. http://www.wormbook.org/chapters/www_celegansintro/celegansintro.html#sec5.2

9. The pharynx of *Caenorhabditis elegans*. *Philos Trans R Soc Lond B Biol Sci*. 1976;275(938):299-325. doi:10.1098/rstb.1976.0085

10. The structure of the nervous system of the nematode *Caenorhabditis elegans*. *Philos Trans R Soc Lond B Biol Sci*. 1986;314(1165):1-340. doi:10.1098/rstb.1986.0056

11. The C. elegans intestine. In: *WormBook*. ; 2007:1-36. http://www.wormbook.org/chapters/www_intestine/intestine.html

12. Dimov I, Maduro MF. The C. elegans intestine: organogenesis, digestion, and physiology. *Cell Tissue Res*. 2019;377(3):383-396. doi:10.1007/s00441-019-03036-4

13. Gordon K. Recent Advances in the Genetic, Anatomical, and Environmental Regulation of the C. elegans Germ Line Progenitor Zone. *J Dev Biol*. 2020;8(3):14. doi:10.3390/jdb8030014

14. Lints R, Hall DH. WormAtlas Hermaphrodite Handbook - Reproductive System - Egg-laying Apparatus. Herndon LA, ed. *WormAtlas*. Published online July 2004. doi:10.3908/wormatlas.1.24

15. Lints R, Hall DH. WormAtlas Hermaphrodite Handbook - Reproductive System - Somatic Gonad. Herndon LA, ed. *WormAtlas*. Published online April 2004. doi:10.3908/wormatlas.1.22

16. Hubbard EJ. Introduction to the germ line. *WormBook*. Published online 2005. doi:10.1895/wormbook.1.18.1

17. Byerly L, Cassada RC, Russell RL. The life cycle of the nematode Caenorhabditis elegans. *Dev Biol*. 1976;51(1):23-33. doi:10.1016/0012-1606(76)90119-6

18. Cassada RC, Russell RL. The dauerlarva, a post-embryonic developmental variant of the nematode Caenorhabditis elegans. *Dev Biol*. 1975;46(2):326-342. doi:10.1016/0012-1606(75)90109-8

19. Hulme SE, Whitesides GM. Chemistry and the Worm: Caenorhabditis elegans as a Platform for Integrating Chemical and Biological Research. *Angew Chem Int Ed*. 2011;50(21):4774-4807. doi:10.1002/anie.201005461

20. Singson A. Sydney Brenner: The birth of a model organism and the worm's connection to reproductive biology. *Mol Reprod Dev*. 2019;86(8):926-927. doi:10.1002/mrd.23176

21. Dyczkowska A, Chabowska-Kita A. Caenorhabditis elegans as a model organism in obesity research. *BioTechnologia*. 2021;102(3):337-362. doi:10.5114/bta.2021.109094

22. Kumar S, Kaur S, Seem K, Kumar S, Mohapatra T. Understanding 3D Genome Organization and Its Effect on Transcriptional Gene Regulation Under Environmental Stress in Plant: A Chromatin Perspective. *Front Cell Dev Biol*. 2021;9:774719. doi:10.3389/fcell.2021.774719

23. Jha RK, Levens D, Kouzine F. Mechanical determinants of chromatin topology and gene expression. *Nucleus*. 2022;13(1):95-116. doi:10.1080/19491034.2022.2038868

24. Fyodorov DV, Zhou BR, Skoultchi AI, Bai Y. Emerging roles of linker histones in regulating chromatin structure and function. *Nat Rev Mol Cell Biol*. 2018;19(3):192-206. doi:10.1038/nrm.2017.94

25. Gill J, Kumar A, Sharma A. Structural comparisons reveal diverse binding modes between nucleosome assembly proteins and histones. *Epigenetics Chromatin*. 2022;15(1):20. doi:10.1186/s13072-022-00452-9

26. Baxevanis A. Histone Sequence Database: a compilation of highly-conserved nucleoprotein sequences. *Nucleic Acids Res*. 1996;24(1):245-247. doi:10.1093/nar/24.1.245

27. Marino-Ramirez L, Levine KM, Morales M, et al. The Histone Database: an integrated resource for histones and histone fold-containing proteins. *Database*. 2011;2011(0):bar048-bar048. doi:10.1093/database/bar048

28. Gebala M, Johnson S, Narlikar G, Herschlag D. *Ion Counting Demonstrates a High Electrostatic Potential of the Nucleosome*. Biophysics; 2019. doi:10.1101/514471

29. Luger K, Mäder AW, Richmond RK, Sargent DF, Richmond TJ. Crystal structure of the nucleosome core particle at 2.8 Å resolution. *Nature*. 1997;389(6648):251-260. doi:10.1038/38444

30. Ma Y, Kanakousaki K, Buttitta L. How the cell cycle impacts chromatin architecture and influences cell fate. *Front Genet*. 2015;6. doi:10.3389/fgene.2015.00019

31. Wu C, Bassett A, Travers A. A variable topology for the 30-nm chromatin fibre. *EMBO Rep*. 2007;8(12):1129-1134. doi:10.1038/sj.embor.7401115

32. Hansen JC, Connolly M, McDonald CJ, et al. The 10-nm chromatin fiber and its relationship to interphase chromosome organization. *Biochem Soc Trans*. 2018;46(1):67-76. doi:10.1042/BST20170101

33. Kadauke S, Blobel GA. Chromatin loops in gene regulation. *Biochim Biophys Acta BBA - Gene Regul Mech*. 2009;1789(1):17-25. doi:10.1016/j.bbagrm.2008.07.002

34. Hansen AS, Cattoglio C, Darzacq X, Tjian R. Recent evidence that TADs and chromatin loops are dynamic structures. *Nucleus*. 2018;9(1):20-32. doi:10.1080/19491034.2017.1389365

35. McArthur E, Capra JA. Topologically associating domain boundaries that are stable across diverse cell types are evolutionarily constrained and enriched for heritability. *Am J Hum Genet*. 2021;108(2):269-283. doi:10.1016/j.ajhg.2021.01.001

36. Cremer T, Cremer C. Chromosome territories, nuclear architecture and gene regulation in mammalian cells. *Nat Rev Genet*. 2001;2(4):292-301. doi:10.1038/35066075

37. Hübner MR, Spector DL. Chromatin Dynamics. *Annu Rev Biophys*. 2010;39(1):471-489. doi:10.1146/annurev.biophys.093008.131348

38. Hancock R. Structure of Metaphase Chromosomes: A Role for Effects of Macromolecular Crowding. Karbstein K, ed. *PLoS ONE*. 2012;7(4):e36045. doi:10.1371/journal.pone.0036045

39. Tamaru H. Confining euchromatin/heterochromatin territory: *jumonji* crosses the line. *Genes Dev*. 2010;24(14):1465-1478. doi:10.1101/gad.1941010

40. Huisinga KL, Brower-Toland B, Elgin SCR. The contradictory definitions of heterochromatin: transcription and silencing. *Chromosoma*. 2006;115(2):110-122. doi:10.1007/s00412-006-0052-x

41. Babu A, Verma RS. Chromosome Structure: Euchromatin and Heterochromatin. In: *International Review of Cytology*. Vol 108. Elsevier; 1987:1-60. doi:10.1016/S0074-7696(08)61435-7

42. Klocko AD, Ormsby T, Galazka JM, et al. Normal chromosome conformation depends on subtelomeric facultative heterochromatin in *Neurospora crassa*. *Proc Natl Acad Sci*. 2016;113(52):15048-15053. doi:10.1073/pnas.1615546113

43. Chantalat S, Depaux A, Héry P, et al. Histone H3 trimethylation at lysine 36 is associated with constitutive and facultative heterochromatin. *Genome Res*. 2011;21(9):1426-1437. doi:10.1101/gr.118091.110

44. Jamieson K, Wiles ET, McNaught KJ, et al. Loss of HP1 causes depletion of H3K27me3 from facultative heterochromatin and gain of H3K27me2 at constitutive heterochromatin. *Genome Res*. 2016;26(1):97-107. doi:10.1101/gr.194555.115

45. Watanabe S, Radman-Livaja M, Rando OJ, Peterson CL. A Histone Acetylation Switch Regulates H2A.Z Deposition by the SWR-C Remodeling Enzyme. *Science*. 2013;340(6129):195-199. doi:10.1126/science.1229758

46. Nocetti N, Whitehouse I. Nucleosome repositioning underlies dynamic gene expression. *Genes Dev*. 2016;30(6):660-672. doi:10.1101/gad.274910.115

47. Bannister AJ, Kouzarides T. Regulation of chromatin by histone modifications. *Cell Res*. 2011;21(3):381-395. doi:10.1038/cr.2011.22

48. Felsenfeld G. A Brief History of Epigenetics. *Cold Spring Harb Perspect Biol*. 2014;6(1):a018200-a018200. doi:10.1101/cshperspect.a018200

49. Berger SL, Kouzarides T, Shiekhattar R, Shilatifard A. An operational definition of epigenetics: Figure 1. *Genes Dev*. 2009;23(7):781-783. doi:10.1101/gad.1787609

50. Dupont C, Armant D, Brenner C. Epigenetics: Definition, Mechanisms and Clinical Perspective. *Semin Reprod Med*. 2009;27(05):351-357. doi:10.1055/s-0029-1237423

51. Moosavi A, Motevalizadeh Ardekani A. Role of Epigenetics in Biology and Human Diseases. *Iran Biomed J*. 2016;(5):246-258. doi:10.22045/ibj.2016.01

52. LA EPIGENÉTICA. SUS MECANISMOS Y SIGNIFICADO EN LA REGULACIÓN GÉNICA. *Cuad Bioét*. 2020;(31(103)). doi:10.30444/CB.79

53. Meaney MJ. Epigenetics and the Biological Definition of Gene × Environment Interactions. *Child Dev*. 2010;81(1):41-79. doi:10.1111/j.1467-8624.2009.01381.x

54. An W. Histone acetylation and methylation: combinatorial players for transcriptional regulation. *Subcell Biochem*. 2007;41:351-369.

55. Handy DE, Castro R, Loscalzo J. Epigenetic Modifications: Basic Mechanisms and Role in Cardiovascular Disease. *Circulation*. 2011;123(19):2145-2156. doi:10.1161/CIRCULATIONAHA.110.956839

56. Verdone L. Histone acetylation in gene regulation. *Brief Funct Genomic Proteomic*. 2006;5(3):209-221. doi:10.1093/bfgp/ell028

57. Lucas X, Wohlwend D, Hügle M, et al. 4-Acyl Pyrroles: Mimicking Acetylated Lysines in Histone Code Reading. *Angew Chem Int Ed*. 2013;52(52):14055-14059. doi:10.1002/anie.201307652

58. Shahid Z, Simpson B, Miao KH, Singh G. Genetics, Histone Code. In: *StatPearls*. StatPearls Publishing; 2023. Accessed October 9, 2023. http://www.ncbi.nlm.nih.gov/books/NBK538477/

59. Greer EL, Shi Y. Histone methylation: a dynamic mark in health, disease and inheritance. *Nat Rev Genet*. 2012;13(5):343-357. doi:10.1038/nrg3173

60. Wan QL, Meng X, Wang C, et al. Histone H3K4me3 modification is a transgenerational epigenetic signal for lipid metabolism in Caenorhabditis elegans. *Nat Commun*. 2022;13(1):768. doi:10.1038/s41467-022-28469-4

61. Singh BN, Zhang G, Hwa YL, Li J, Dowdy SC, Jiang SW. Nonhistone protein acetylation as cancer therapy targets. *Expert Rev Anticancer Ther*. 2010;10(6):935-954. doi:10.1586/era.10.62

62. Shvedunova M, Akhtar A. Modulation of cellular processes by histone and non-histone protein acetylation. *Nat Rev Mol Cell Biol*. 2022;23(5):329-349. doi:10.1038/s41580-021-00441-y

63. Li Y, Huang H, Zhu M, Bai H, Huang X. Roles of the MYST Family in the Pathogenesis of Alzheimer's Disease via Histone or Non-histone Acetylation. *Aging Dis*. 2021;12(1):132. doi:10.14336/AD.2020.0329

64. Botrugno OA, Robert T, Vanoli F, Foiani M, Minucci S. Molecular Pathways: Old Drugs Define New Pathways: Non-Histone Acetylation at the Crossroads of the DNA Damage Response and Autophagy. *Clin Cancer Res*. 2012;18(9):2436-2442. doi:10.1158/1078-0432.CCR-11-0767

65. Liu H, Li Z, Yang Q, et al. Substrate docking–mediated specific and efficient lysine methylation by the SET domain–containing histone methyltransferase SETD7. *J Biol Chem*. 2019;294(36):13355-13365. doi:10.1074/jbc.RA119.009630

66. Zhang X, Wen H, Shi X. Lysine methylation: beyond histones. *Acta Biochim Biophys Sin*. 2012;44(1):14-27. doi:10.1093/abbs/gmr100

67. Biggar KK, Li SSC. Non-histone protein methylation as a regulator of cellular signalling and function. *Nat Rev Mol Cell Biol*. 2015;16(1):5-17. doi:10.1038/nrm3915

68. Zhao LN, Guccione E, Kaldis P. Proof-of-Concept Method to Study Uncharacterized Methyltransferases Using PRDM15. *Int J Mol Sci*. 2023;24(2):1327. doi:10.3390/ijms24021327

69. Chiang C, Yang H, Zhu L, et al. The Epigenetic Regulation of Nonhistone Proteins by SETD7: New Targets in Cancer. *Front Genet*. 2022;13:918509. doi:10.3389/fgene.2022.918509

70. Chopra A, Cho WC, Willmore WG, Biggar KK. Hypoxia-Inducible Lysine Methyltransferases: G9a and GLP Hypoxic Regulation, Non-histone Substrate Modification, and Pathological Relevance. *Front Genet*. 2020;11:579636. doi:10.3389/fgene.2020.579636

71. Rao RA, Ketkar AA, Kedia N, et al. KMT1 family methyltransferases regulate heterochromatin–nuclear periphery tethering via histone and non-histone protein methylation. *EMBO Rep*. 2019;20(5):e43260. doi:10.15252/embr.201643260

72. Lee JM, Kim H, Im H, Baek H ji. Abstract 1493: ROS inhibits enzymatic activation of PRMT5 and increases the protein stability of tumor suppressors as non-histone substrates in liver cancer. *Cancer Res*. 2023;83(7_Supplement):1493-1493. doi:10.1158/1538-7445.AM2023-1493

73. Dillon SC, Zhang X, Trievel RC, Cheng X. [No title found]. *Genome Biol*. 2005;6(8):227. doi:10.1186/gb-2005-6-8-227

74. Zhou H, Liu Y, Liang Y, et al. The function of histone lysine methylation related SET domain group proteins in plants. *Protein Sci*. 2020;29(5):1120-1137. doi:10.1002/pro.3849

75. Jenuwein T, Laible G, Dorn R, Reuter G. SET domain proteins modulate chromatin domains in eu- and heterochromatin. *Cell Mol Life Sci CMLS*. 1998;54(1):80-93. doi:10.1007/s000180050127

76. Zhang X, Tamaru H, Khan SI, et al. Structure of the Neurospora SET Domain Protein DIM-5, a Histone H3 Lysine Methyltransferase. *Cell*. 2002;111(1):117-127. doi:10.1016/S0092-8674(02)00999-6

77. Min J, Zhang X, Cheng X, Grewal SIS, Xu RM. Structure of the SET domain histone lysine methyltransferase Clr4. *Nat Struct Biol*. Published online October 21, 2002. doi:10.1038/nsb860

78. Weirich S, Khella MS, Jeltsch A. Structure, Activity and Function of the Suv39h1 and Suv39h2 Protein Lysine Methyltransferases. *Life*. 2021;11(7):703. doi:10.3390/life11070703

79. Schwartz-Orbach L, Zhang C, Sidoli S, et al. Caenorhabditis elegans nuclear RNAi factor SET-32 deposits the transgenerational histone modification, H3K23me3. *eLife*. 2020;9:e54309. doi:10.7554/eLife.54309

80. Abay-Nørgaard S, Attianese B, Boreggio L, Salcini AE. Regulators of H3K4 methylation mutated in neurodevelopmental disorders control axon guidance in *C. elegans*. *Development*. Published online January 1, 2020:dev.190637. doi:10.1242/dev.190637

81. Engert CG, Droste R, Van Oudenaarden A, Horvitz HR. A Caenorhabditis elegans protein with a PRDM9-like SET domain localizes to chromatin-associated foci and promotes spermatocyte gene expression, sperm production and fertility. Ahringer J, ed. *PLOS Genet*. 2018;14(4):e1007295. doi:10.1371/journal.pgen.1007295

82. Fahy E, Cotter D, Sud M, Subramaniam S. Lipid classification, structures and tools. *Biochim Biophys Acta BBA - Mol Cell Biol Lipids*. 2011;1811(11):637-647. doi:10.1016/j.bbalip.2011.06.009

83. Abeyrathne EDNS, Nam KC, Huang X, Ahn DU. Egg yolk lipids: separation, characterization, and utilization. *Food Sci Biotechnol*. 2022;31(10):1243-1256. doi:10.1007/s10068-022-01138-4

84. Walczak J, Bocian S, Kowalkowski T, Trziszka T, Buszewski B. Determination of Omega Fatty Acid Profiles in Egg Yolk by HILIC-LC-MS and GC-MS. *Food Anal Methods*. 2017;10(5):1264-1272. doi:10.1007/s12161-016-0655-7

85. Schwingshackl L, Hoffmann G. Monounsaturated Fatty Acids and Risk of Cardiovascular Disease: Synopsis of the Evidence Available from Systematic Reviews and Meta-Analyses. *Nutrients*. 2012;4(12):1989-2007. doi:10.3390/nu4121989

86. Mashek DG, Wu C. MUFAs. *Adv Nutr*. 2015;6(3):276-277. doi:10.3945/an.114.005926

87. Rubio-Tomás T, Tavernarakis N. Lipid metabolism and ageing in Caenorhabditis elegans: a complex interplay. *Biogerontology*. 2022;23(5):541-557. doi:10.1007/s10522-022-09989-4

88. Mutlu AS, Duffy J, Wang MC. Lipid metabolism and lipid signals in aging and longevity. *Dev Cell*. 2021;56(10):1394-1407. doi:10.1016/j.devcel.2021.03.034

89. Chandel NS. Lipid Metabolism. *Cold Spring Harb Perspect Biol*. 2021;13(9):a040576. doi:10.1101/cshperspect.a040576

90. Wymann MP, Schneiter R. Lipid signalling in disease. *Nat Rev Mol Cell Biol*. 2008;9(2):162-176. doi:10.1038/nrm2335

91. Keleher MR, Zaidi R, Hicks L, et al. A high-fat diet alters genome-wide DNA methylation and gene expression in SM/J mice. *BMC Genomics*. 2018;19(1):888. doi:10.1186/s12864-018-5327-0

92. Tavernarakis N. Inflammation brakes mitochondrial metabolism in obesity. *Nat Immunol*. 2020;21(10):1143-1145. doi:10.1038/s41590-020-0780-8

93. Vucetic Z, Kimmel J, Totoki K, Hollenbeck E, Reyes TM. Maternal High-Fat Diet Alters Methylation and Gene Expression of Dopamine and Opioid-Related Genes. *Endocrinology*. 2010;151(10):4756-4764. doi:10.1210/en.2010-0505

94. Ciccarone F, Castelli S, Ioannilli L, Ciriolo MR. High Dietary Fat Intake Affects DNA Methylation/Hydroxymethylation in Mouse Heart: Epigenetic Hints for Obesity-Related Cardiac Dysfunction. *Mol Nutr Food Res*. 2019;63(4):1800970. doi:10.1002/mnfr.201800970

95. Hajri T, Zaiou M, Fungwe TV, Ouguerram K, Besong S. Epigenetic Regulation of Peroxisome Proliferator-Activated Receptor Gamma Mediates High-Fat Diet-Induced Non-Alcoholic Fatty Liver Disease. *Cells*. 2021;10(6):1355. doi:10.3390/cells10061355

96. Aagaard-Tillery KM, Grove K, Bishop J, et al. Developmental origins of disease and determinants of chromatin structure: maternal diet modifies the primate fetal epigenome. *J Mol Endocrinol*. 2008;41(2):91-102. doi:10.1677/JME-08-0025

97. Dunn GA, Bale TL. Maternal High-Fat Diet Effects on Third-Generation Female Body Size via the Paternal Lineage. *Endocrinology*. 2011;152(6):2228-2236. doi:10.1210/en.2010-1461

98. Terashima M, Barbour S, Ren J, Yu W, Han Y, Muegge K. Effect of high fat diet on paternal sperm histone distribution and male offspring liver gene expression. *Epigenetics*. 2015;10(9):861-871. doi:10.1080/15592294.2015.1075691

99. Chung KW. Advances in Understanding of the Role of Lipid Metabolism in Aging. *Cells*. 2021;10(4):880. doi:10.3390/cells10040880

100. Fernandis AZ, Wenk MR. Membrane lipids as signaling molecules. *Curr Opin Lipidol*. 2007;18(2):121-128. doi:10.1097/MOL.0b013e328082e4d5

101. Butruille L, Marousez L, Pourpe C, et al. Maternal high-fat diet during suckling programs visceral adiposity and epigenetic regulation of adipose tissue stearoyl-CoA desaturase-1 in offspring. *Int J Obes*. 2019;43(12):2381-2393. doi:10.1038/s41366-018-0310-z

102. Huang CJ, McAllister MJ, Slusher AL, Webb HE, Mock JT, Acevedo EO. Obesity-Related Oxidative Stress: the Impact of Physical Activity and Diet Manipulation. *Sports Med - Open*. 2015;1(1):32. doi:10.1186/s40798-015-0031-y

103. Hildebrandt X, Ibrahim M, Peltzer N. Cell death and inflammation during obesity: "Know my methods, WAT(son)." *Cell Death Differ*. 2023;30(2):279-292. doi:10.1038/s41418-022-01062-4

104. Ogrodnik M, Zhu Y, Langhi LGP, et al. Obesity-Induced Cellular Senescence Drives Anxiety and Impairs Neurogenesis. *Cell Metab*. 2019;29(5):1061-1077.e8. doi:10.1016/j.cmet.2018.12.008

105. Jakubczyk K, Dec K, Kałduńska J, Kawczuga D, Kochman J, Janda K. Reactive oxygen species - sources, functions, oxidative damage. *Pol Merkur Lek Organ Pol Tow Lek*. 2020;48(284):124-127.

106. Rigoulet M, Yoboue ED, Devin A. Mitochondrial ROS Generation and Its Regulation: Mechanisms Involved in H_2O_2 Signaling. *Antioxid Redox Signal*. 2011;14(3):459-468. doi:10.1089/ars.2010.3363

107. Magnani F, Mattevi A. Structure and mechanisms of ROS generation by NADPH oxidases. *Curr Opin Struct Biol*. 2019;59:91-97. doi:10.1016/j.sbi.2019.03.001

108. Sarniak A, Lipińska J, Tytman K, Lipińska S. Endogenous mechanisms of reactive oxygen species (ROS) generation. *Postępy Hig Med Dośw*. 2016;70:1150-1165. doi:10.5604/17322693.1224259

109. Juan CA, Pérez De La Lastra JM, Plou FJ, Pérez-Lebeña E. The Chemistry of Reactive Oxygen Species (ROS) Revisited: Outlining Their Role in Biological Macromolecules (DNA, Lipids and Proteins) and Induced Pathologies. *Int J Mol Sci*. 2021;22(9):4642. doi:10.3390/ijms22094642

110. He L, He T, Farrar S, Ji L, Liu T, Ma X. Antioxidants Maintain Cellular Redox Homeostasis by Elimination of Reactive Oxygen Species. *Cell Physiol Biochem*. 2017;44(2):532-553. doi:10.1159/000485089

111. Léger C, Bertrand P. Direct Electrochemistry of Redox Enzymes as a Tool for Mechanistic Studies. *Chem Rev*. 2008;108(7):2379-2438. doi:10.1021/cr0680742

112. Du X, Zhu Y, Peng Z, et al. High concentrations of fatty acids and β-hydroxybutyrate impair the growth hormone-mediated hepatic JAK2-STAT5 pathway in clinically ketotic cows. *J Dairy Sci*. 2018;101(4):3476-3487. doi:10.3168/jds.2017-13234

113. Derosa G, Sahebkar A, Maffioli P. The role of various peroxisome proliferator-activated receptors and their ligands in clinical practice. *J Cell Physiol*. 2018;233(1):153-161. doi:10.1002/jcp.25804

114. Tan BL, Norhaizan ME. Effect of High-Fat Diets on Oxidative Stress, Cellular Inflammatory Response and Cognitive Function. *Nutrients*. 2019;11(11):2579. doi:10.3390/nu11112579

115. Lu C, Thompson CB. Metabolic Regulation of Epigenetics. *Cell Metab*. 2012;16(1):9-17. doi:10.1016/j.cmet.2012.06.001

116. Ferrari A, Fiorino E, Giudici M, et al. Linking epigenetics to lipid metabolism: Focus on histone deacetylases. *Mol Membr Biol*. 2012;29(7):257-266. doi:10.3109/09687688.2012.729094

117. González-Becerra K, Ramos-Lopez O, Barrón-Cabrera E, et al. Fatty acids, epigenetic mechanisms and chronic diseases: a systematic review. *Lipids Health Dis*. 2019;18(1):178. doi:10.1186/s12944-019-1120-6

118. Li X, Li Q, Ju L, et al. Deficiency of Histone Methyltransferase SET Domain-Containing 2 in Liver Leads to Abnormal Lipid Metabolism and HCC. *Hepatology*. 2021;73(5):1797-1815. doi:10.1002/hep.31594

119. Papsdorf K, Brunet A. Linking Lipid Metabolism to Chromatin Regulation in Aging. *Trends Cell Biol*. 2019;29(2):97-116. doi:10.1016/j.tcb.2018.09.004

120. Search Strains - Caenorhabditis Genetics Center (CGC) - College of Biological Sciences. Accessed October 19, 2023. https://cgc.umn.edu/strain/search?st1=VC997&sf1=all&xt1=&xf1=all&st2=&sf2=strain&xt2=&xf2=strain&st3=&sf3=genotype&xt3=&xf3=genotype&st4=&sf4=species&xt4=&xf4=species

121. Search Strains - Caenorhabditis Genetics Center (CGC) - College of Biological Sciences. Accessed October 19, 2023. https://cgc.umn.edu/strain/search?st1=VC983&sf1=all&xt1=&xf1=all&st2=&sf2=strain&xt2=&xf2=strain&st3=&sf3=genotype&xt3=&xf3=genotype&st4=&sf4=species&xt4=&xf4=species

122. Search Strains - Caenorhabditis Genetics Center (CGC) - College of Biological Sciences. Accessed October 19, 2023. https://cgc.umn.edu/strain/search?st1=VC767&sf1=all&xt1=&xf1=all&st2=&sf2=strain&xt2=&xf2=strain&st3=&sf3=genotype&xt3=&xf3=genotype&st4=&sf4=species&xt4=&xf4=species

123. Search Strains - Caenorhabditis Genetics Center (CGC) - College of Biological Sciences. Accessed October 19, 2023. https://cgc.umn.edu/strain/search?st1=VC719&sf1=all&xt1=&xf1=all&st2=&sf2=strain&xt2=&xf2=strain&st3=&sf3=genotype&xt3=&xf3=genotype&st4=&sf4=species&xt4=&xf4=species

124. Search Strains - Caenorhabditis Genetics Center (CGC) - College of Biological Sciences. Accessed October 19, 2023. https://cgc.umn.edu/strain/search?st1=RG3241&sf1=all&xt1=&xf1=all&st2=&sf2=strain&xt2=&xf2=strain&st3=&sf3=genotype&xt3=&xf3=genotype&st4=&sf4=species&xt4=&xf4=species

125. Schindelin J, Arganda-Carreras I, Frise E, et al. Fiji: an open-source platform for biological-image analysis. *Nat Methods*. 2012;9(7):676-682. doi:10.1038/nmeth.2019

126. Dues DJ, Schaar CE, Johnson BK, et al. Uncoupling of oxidative stress resistance and lifespan in long-lived isp-1 mitochondrial mutants in Caenorhabditis elegans. *Free Radic Biol Med*. 2017;108:362-373. doi:10.1016/j.freeradbiomed.2017.04.004

127. Li TY, Sleiman MB, Li H, et al. The transcriptional coactivator CBP/p300 is an evolutionarily conserved node that promotes longevity in response to mitochondrial stress. *Nat Aging*. 2021;1(2):165-178. doi:10.1038/s43587-020-00025-z

128. Barrett LN, Westerheide SD. The CBP-1/p300 Lysine Acetyltransferase Regulates the Heat Shock Response in C. elegans. *Front Aging*. 2022;3:861761. doi:10.3389/fragi.2022.861761

129. Bernstein BE, Humphrey EL, Erlich RL, et al. Methylation of histone H3 Lys 4 in coding regions of active genes. *Proc Natl Acad Sci*. 2002;99(13):8695-8700. doi:10.1073/pnas.082249499

130. Greer EL, Maures TJ, Hauswirth AG, et al. Members of the H3K4 trimethylation complex regulate lifespan in a germline-dependent manner in C. elegans. *Nature*. 2010;466(7304):383-387. doi:10.1038/nature09195

131. Hachinohe M, Hanaoka F, Masumoto H. Hst3 and Hst4 histone deacetylases regulate replicative lifespan by preventing genome instability in Saccharomyces cerevisiae: Hst3 and Hst4 histone deacetylases regulate replicative lifespan. *Genes Cells*. 2011;16(4):467-477. doi:10.1111/j.1365-2443.2011.01493.x

132. Santos-Rosa H, Schneider R, Bannister AJ, et al. Active genes are tri-methylated at K4 of histone H3. *Nature*. 2002;419(6905):407-411. doi:10.1038/nature01080

133. Wang K, Liu H, Hu Q, et al. Epigenetic regulation of aging: implications for interventions of aging and diseases. *Signal Transduct Target Ther*. 2022;7(1):374. doi:10.1038/s41392-022-01211-8

134. Franco-Juárez B, Gómez-Manzo S, Hernández-Ochoa B, et al. Effects of High Dietary Carbohydrate and Lipid Intake on the Lifespan of C. elegans. *Cells*. 2021;10(9):2359. doi:10.3390/cells10092359

135. Hashmi S, Wang Y, Parhar RS, et al. A C. elegans model to study human metabolic regulation. *Nutr Metab*. 2013;10(1):31. doi:10.1186/1743-7075-10-31